



#### ANNUAL REVIEWS **Further**

Click [here](#) to view this article's online features:

- Download figures as PPT slides
- Navigate linked references
- Download citations
- Explore related articles
- Search keywords

# Microbial Rhodopsins: Diversity, Mechanisms, and Optogenetic Applications

Elena G. Govorunova, Oleg A. Sineshchekov, Hai Li,  
and John L. Spudich

Center for Membrane Biology, Department of Biochemistry and Molecular Biology, McGovern Medical School, University of Texas Health Science Center at Houston, Houston, Texas 77030;  
email: [Elena.G.Govorunova@uth.tmc.edu](mailto:Elena.G.Govorunova@uth.tmc.edu), [Oleg.A.Sineshchekov@uth.tmc.edu](mailto:Oleg.A.Sineshchekov@uth.tmc.edu),  
[Hai.Li@uth.tmc.edu](mailto:Hai.Li@uth.tmc.edu), [John.L.Spudich@uth.tmc.edu](mailto:John.L.Spudich@uth.tmc.edu)

Annu. Rev. Biochem. 2017. 86:845–72

First published as a Review in Advance on  
March 9, 2017

The *Annual Review of Biochemistry* is online at  
[biochem.annualreviews.org](http://biochem.annualreviews.org)

<https://doi.org/10.1146/annurev-biochem-101910-144233>

Copyright © 2017 by Annual Reviews.  
All rights reserved

## Keywords

retinylidene proteins, ion pumps, photosensors, cation channelrhodopsins, anion channelrhodopsins, optogenetics

## Abstract

Microbial rhodopsins are a family of photoactive retinylidene proteins widespread throughout the microbial world. They are notable for their diversity of function, using variations of a shared seven-transmembrane helix design and similar photochemical reactions to carry out distinctly different light-driven energy and sensory transduction processes. Their study has contributed to our understanding of how evolution modifies protein scaffolds to create new protein chemistry, and their use as tools to control membrane potential with light is fundamental to optogenetics for research and clinical applications. We review the currently known functions and present more in-depth assessment of three functionally and structurally distinct types discovered over the past two years: (*a*) anion channelrhodopsins (ACRs) from cryptophyte algae, which enable efficient optogenetic neural suppression; (*b*) cryptophyte cation channelrhodopsins (CCRs), structurally distinct from the green algae CCRs used extensively for neural activation and from cryptophyte ACRs; and (*c*) enzymorhodopsins, with light-gated guanylyl cyclase or kinase activity promising for optogenetic control of signal transduction.

## Contents

INTRODUCTION .....	846
Microbial Rhodopsins in Nature .....	846
Use as Optogenetics Tools .....	847
Scope of the Review .....	849
THE KNOWN MOLECULAR FUNCTIONS	
OF MICROBIAL RHODOPSINS .....	849
Light Energy Capture by Light-Driven Ion Pumps .....	849
Sensory Rhodopsins: Diverse Signaling Mechanisms .....	852
FUTURE PROSPECTS IN RESEARCH AND CLINICAL OPTOGENETICS ...	864

## INTRODUCTION

### Microbial Rhodopsins in Nature

The microbial rhodopsin family comprises >7,000 photochemically reactive proteins in prokaryotes and lower eukaryotes found throughout the oceans from the tropics to the arctic, in lakes and rivers, in soil, and on the leaf surfaces of plants (**Figure 1**). Family members share a membrane-embedded seven-helix architecture that forms an internal pocket for the chromophore retinal bound in a protonated Schiff base linkage to the  $\epsilon$ -amino group of a lysyl residue in the middle of the 7th helix. Microbial rhodopsins provide a vivid example of evolution modifying a

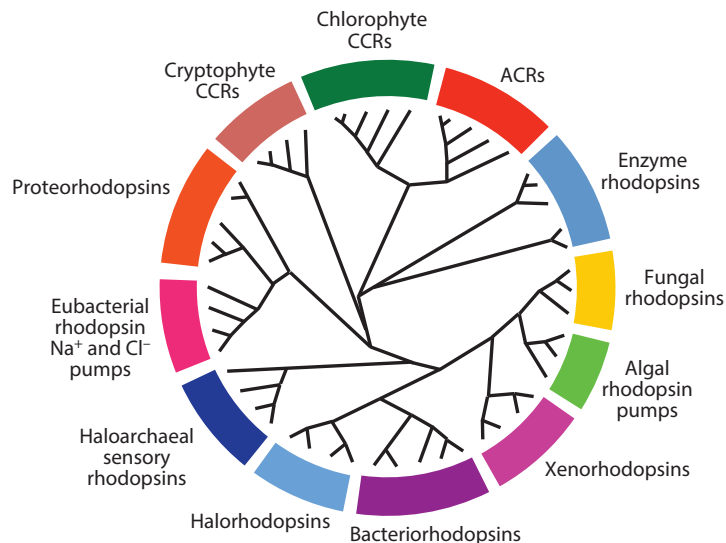


**Figure 1**

A cladogram of the microbial rhodopsin superfamily. For a list of sequences, accession numbers, and source organisms see **Supplemental Table 1**. Follow the **Supplemental Material** link from the Annual Reviews home page at <http://www.annualreviews.org>. Abbreviations: ACRs, anion channelrhodopsins; CCRs, cation channelrhodopsins.

single protein scaffold to produce diverse new chemical functions. Photochemical reactions energized by photoisomerization of the retinylidene chromophore drive distinctly different processes in different microbial rhodopsins. Their biological functions fall into two categories: (a) photoenergy transducers that convert light into electrochemical potential to energize cells, namely light-driven ion pumps catalyzing outward active transport of protons, inward chloride transport, and outward sodium transport; (b) photosensory receptors that use light to gain information about the environment to regulate cell processes (**Figure 2**). Known modes of microbial sensory rhodopsin signaling are protein–protein interaction with membrane-embedded transducers, interaction of their cytoplasmic domain with soluble transducer proteins, enzymatic activity encoded in their cytoplasmic domain, and signaling by light-gated passive ion channel conduction.

The microbial rhodopsins are so named because of their structural similarity to animal visual pigments, such as mammalian rod rhodopsin, which also comprise seven transmembrane helices forming an interior protonated retinylidene Schiff base chromophore also linked to a lysyl residue in the 7th helix. For both microbial and animal rhodopsins, their apoproteins are referred to as opsins and, when complexed with the retinal moiety, rhodopsins. Microbial rhodopsins and animal rhodopsins exhibit mechanistic as well as structural similarities but no sequence homology. On the basis of their distinctly different phylogeny, they have been designated type 1 and type 2 rhodopsins, respectively (1). The question of whether types 1 and 2 derive from convergent evolution or diverged from a common seven-helix retinylidene ancestor is still unresolved, but the latter possibility has recently received new support (2).

## Use as Optogenetics Tools

Since their discovery in the 1970s and 1980s, the temporal and spatial precision available from using light as a stimulus and the convenience of having a natural spectroscopic reporter group in the photoactive site (i.e., the retinylidene chromophore) have enabled microbial rhodopsins to contribute substantially to our understanding of membrane protein structure/function, photochemistry, bioenergetics, sensory signaling, protein evolution, and the diversity of modes of interaction of organisms with light. One of their most significant contributions is in laying the chemical foundation for the new biotechnology of optogenetics. Optogenetics, an approach that uses light to control cell membrane potential in neurons and other excitable cells, has revolutionized neuroscience research, especially studies of brain function (3, 4). The chemical basis of optogenetics is genetically targeted expression of microbial rhodopsins, whose photochemical reactions enable precise spatial and temporal photocontrol of transmembrane ion currents to regulate neuronal action potentials. This new technology has transformed the study of neural circuitry in flies, worms, rodents, and other animal models and has greatly accelerated the pace of discoveries in brain functions.

Studies of using optogenetics for gene therapy for neurological and cardiac diseases in animal models are promising. Clinical optogenetics is in early stages, and the first human clinical trials for optogenetic restoration of vision in blind individuals with a channelrhodopsin have begun this past year.

Microbial rhodopsins have provided the photochemical basis of optogenetics, with phototaxis receptors from algae with light-gated channel activity being particularly important contributors. Notably, the development of optogenetics is yet one more beautiful example of a revolutionary biotechnology growing out of purely basic research—in this case, research by an international community of skillful and enthusiastic basic scientists studying over decades the photobiology, photochemistry, and photophysics of microbial rhodopsins.

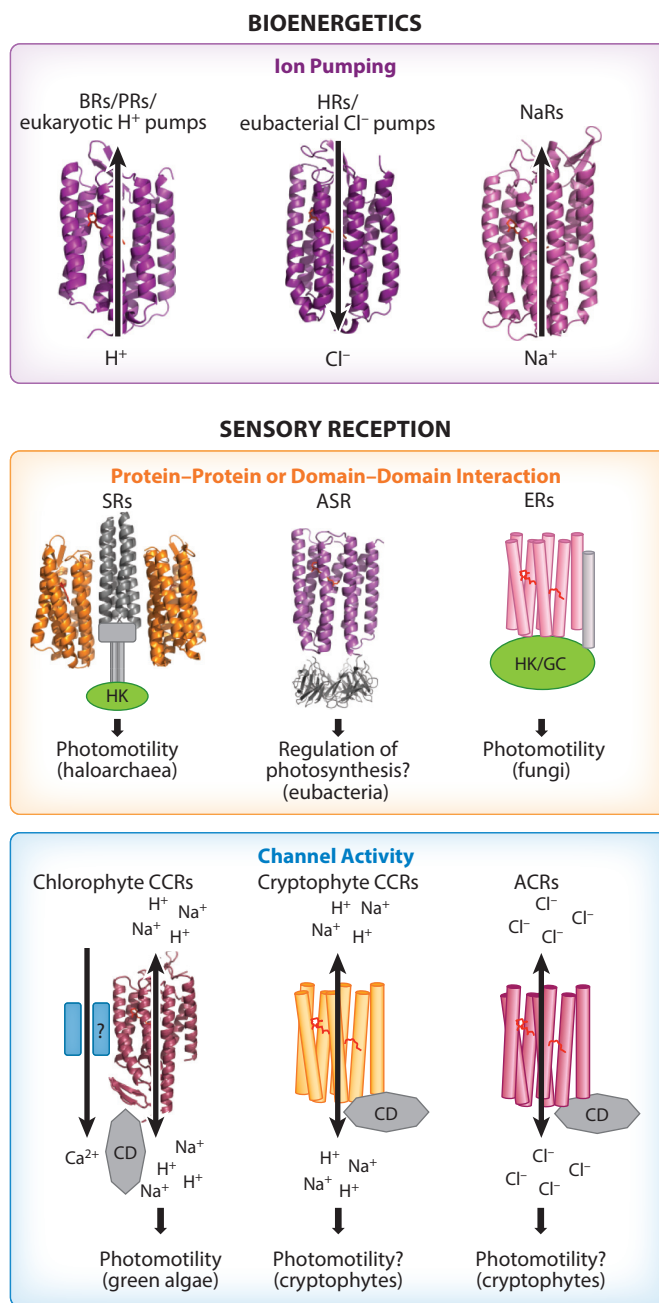


**Figure 2**

Functional types of microbial rhodopsins. All molecules are oriented with their extracellular surface pointing upward. For the molecules shown as ribbons, high-resolution crystal structures have been obtained. Abbreviations: ACRs, anion channelrhodopsins; ASR, *Anabaena* sensory rhodopsin; BRs, bacteriorhodopsins; CCRs, cation channelrhodopsins; CD, cytoplasmic domain; ERs, enzymorhodopsins; GC, guanylyl cyclase; HK, histidine kinase; HRs, halorhodopsins; NaRs,  $Na^+$ -pumping rhodopsins; PRs, proteorhodopsins; SRs, prokaryotic sensory rhodopsins.

## Scope of the Review

Comprehensive reviews have appeared on retinylidene proteins in general (both types 1 and 2) (1, 5) and on various aspects of particular type 1 rhodopsins (6–11; see also references cited in specific sections below). In this focused review, we first briefly cover all of the known molecular functions of microbial rhodopsins, including the history of their discovery and particularly, in some cases, uniquely interesting aspects of their properties that have advanced our understanding of photobiochemistry and photobiology.

Second, we present a more in-depth review of type 1 rhodopsins and new functions discovered in the past two years in this rapidly moving field, namely (*a*) anion channelrhodopsins (ACRs) from cryptophyte algae, notable for their unparalleled efficiency of hyperpolarization and silencing of neural firing; (*b*) cation channelrhodopsins (CCRs) from cryptophyte algae, structurally distinct from the green algae CCRs and closely related to haloarchaeal proton pumps, an example of convergent evolution of channel function via two independent paths; and (*c*) enzymerrhodopsins, microbial rhodopsins with a catalytic domain, specifically in the best understood case a light-gated guanylyl cyclase activity used by a fungus for phototaxis and promising for optogenetic control of cyclic guanosine monophosphate (cGMP) signaling processes.

## THE KNOWN MOLECULAR FUNCTIONS OF MICROBIAL RHODOPSINS

### Light Energy Capture by Light-Driven Ion Pumps

The most abundant and widespread type 1 rhodopsins known are light-driven pumps that carry out vectorial translocation of specific ions across prokaryotic cell membranes, thereby transducing light into electrochemical membrane potential used to power processes such as ATP synthesis, transport of substrates into and out of cells, and cell motility. Light-driven pumps specific for protons were discovered first and account for most of the type 1 rhodopsin genes known. Rhodopsin pumps for chloride and most recently for sodium ions have also been found.

**Proton pumps.** The first discovered type 1 rhodopsin was the proton pump bacteriorhodopsin (BR) in haloarchaea. After three decades of fruitful study of BR, environmental genomics revealed rhodopsin proton pumps in numerous species of marine, freshwater, and soil bacteria and also eukaryotic microorganisms.

**Bacteriorhodopsin.** In the late 1960s Walther Stoeckenius was interested in electron microscopy of the archaeal organism *Halobacterium salinarum* (at that time classified as a bacterium) because of reports that its cytoplasmic membrane may have a subunit structure. However, its unusual surface structure was revealed to be from 2D-crystalline arrays of a then-unknown protein pigment forming purple patches in the cytoplasmic membrane. In the early 1970s Oesterhelt & Stoeckenius (12) discovered that the purple membrane contained a retinylidene proton pump that they named bacteriorhodopsin (BR). Like visual pigments, BR consisted of an apoprotein that formed a pigment with visible absorption upon binding retinal. Within a few years BR gained great importance as a simple single-polypeptide primary transporter obtainable in a stable concentrated form amenable to optical and molecular spectroscopic measurements and crystallography. Indeed it became the first protein in which transmembrane  $\alpha$ -helices were directly observed in a pioneering application of cryo-electron crystallography (13). Close relatives of BR were found in other haloarchaea, such as archaerhodopsin-3 (also known as AR-3 or Arch),

which shows more promiscuous expression in heterologous systems than BR and has found use as a tool for neural photosuppression in optogenetics (14).

**Proteorhodopsins.** Proteorhodopsins (PRs) from proteobacteria, the largest subfamily of microbial rhodopsins, are light-driven proton pumps with the typical carboxylate proton acceptors and donors (Asp-85 and Asp-96 in BR) of haloarchaeal proton pumps. The first PR was discovered by environmental sequencing of Pacific coastal waters (15) followed by several more from Hawaiian surface and deep ocean samples (16). Now thousands of PR genes have been identified in essentially all of the Earth's oceans by shotgun sequencing (17). Estimated from Mediterranean Sea samples, 13% of the bacterial cells in the photic zone contain a PR gene (18). The measured concentration of PRs in picoplankton (16) indicates that solar energy absorption by PRs on the Earth's surface waters continuously converts light energy into transmembrane proton electrochemical potential at a rate of  $\sim 10^{13}$  W, roughly equal to the energy consumption rate of fossil fuels by the human population. Remarkably this significant amount of solar energy capture was completely unknown before 2000 (15), when chlorophyll-based photosynthetic systems were the only known source of energy-transducing membranes in the ocean. Structure/function analysis of PRs revealed a property previously unknown in microbial rhodopsins: oligomeric forms with cross-protomer interactions with the photoactive site of adjacent protomers modulating transport function (19, 20).

**Other proton-pumping rhodopsins.** In addition to large numbers of PRs in proteobacteria, there are PR-related rhodopsins in actinobacteria primarily in freshwater lakes (21) and several examples of PR-like variants termed xanthorhodopsins, unusual in that they contain carotenoid accessory pigments serving as light-harvesting pigments for energy transfer to the retinylidene chromophore (22). Eukaryotic microorganisms, some fungi and algae, also contain rhodopsin proton pumps (23), although the majority of eukaryotic type 1 rhodopsins currently studied have photosensory function.

Recently a type 1 rhodopsin from a deep ocean marine proteobacterium was reported to function as a light-driven inward proton pump when expressed in *Escherichia coli* and cultured mammalian cells (24). The physiological function of an inward proton pump in a bacterium remains an interesting mystery because in contrast to other proton pumps it would dissipate the transmembrane proton electrochemical gradient and hence decrease cellular energy.

**Chloride pumps.** In 1977 Matsuno-Yagi & Mukohata (25) reported the existence of light-induced proton fluxes in a variant of *H. salinarum* cells with little or no BR, and in 1981 Mukohata & Kaji (26) showed that the activity was caused by a distinct pigment they named halorhodopsin (HR). In contrast to BR, which carries out electrogenic ejection of protons from the cell, HR illumination causes a passive influx of protons indicating membrane hyperpolarization by electrogenic transport of another ion. They and other groups suggested HR was a primary  $\text{Na}^+$  pump or a BR-like pigment coupled to a  $\text{H}^+/\text{Na}^+$  antiporter, but Schobert & Lanyi (27) discovered by light-scattering measurements and ion dependencies of photocurrents in cells that HR was an inwardly directed  $\text{Cl}^-$  pump. A dramatic demonstration of the close relationship of the haloarchaeal HR chloride transport and BR proton-pumping mechanisms was the finding that a single mutation of BR, replacement of its protonated Schiff base proton acceptor Asp85 with threonine (which is in the homologous position in HR), converted BR into a light-driven chloride pump (28). Like the proton pump Arch, HR from *Natronomonas pharaonis* (*NpHR*; the first two italicized letters indicate the genus and species name of the source organism) has been used in many studies as an optogenetic suppressor of neural firing (29).

An inwardly directed chloride-pumping rhodopsin (CIR), the primary structure of which shows a phylogenetic lineage very distant from HR, was recently found in a marine bacterium (30, 31). UV-visible absorption measurements indicate that the CIR binds  $\text{Cl}^-$  near the retinal chromophore (32), as is known for HR. A common property of CIR and HR is that the Schiff base remains protonated throughout the pumping cycle, whereas  $\text{Cl}^-$  uptake kinetics differ (32). A crystal structure of the CIR from *Nonlabens marinus* shows greater similarity to the structure of the light-driven  $\text{Na}^+$  pump KR2 from *Krokinobacter* (also known as *Dokdonia*) *eikastus* (33) than to those of archaeal ion pumps, consistent with the convergent evolution of  $\text{Cl}^-$  pumping within the archaeal and eubacterial type 1 rhodopsin subfamilies.

A third version of  $\text{Cl}^-$ -pumping rhodopsins that not only combines structural features of BR and HR but also contains a number of unique residues, was discovered in cyanobacteria (34). In this protein the proton donor residue, Asp96 in BR, is conserved, in contrast to haloarchaeal HRs and CIR. Its functional characterization has just begun but has already suggested a unique mechanism of  $\text{Cl}^-$  transport involving an interplay of  $\text{Cl}^-$  and  $\text{H}^+$  transfers, which is significantly different from that found in HR (A. Harris, A. Hughes-Visentin, M. Saita, T. Resler, R. Maia, F. Sellnau, A.-N. Bondar, J. Heberle, and L.S. Brown, personal communication).

**Sodium pumps.** An outwardly directed sodium ion pumping rhodopsin, named KR2, was discovered in 2013 in the marine flavobacterium *K. eikastus* (35). It was recognized by light-induced  $\text{Na}^+$ -dependent passive  $\text{H}^+$  influx upon expression of the corresponding gene in *E. coli*, as well as by major effects of  $\text{Na}^+$  on the photochemical reaction cycle of the purified protein. KR2 contains the NDQ motif near the retinylidene Schiff base noted in marine eubacteria (36), so named for its contrast with the DTD and DTE motifs in haloarchaeal proton pumps and proteorhodopsins. More than 10 homologs, termed NaRs ( $\text{Na}^+$ -pumping rhodopsins), have been reported (11), and functional studies in *E. coli* cells expressing four different NaRs have been conducted (30, 35, 37, 38). KR2 was shown to outwardly pump  $\text{H}^+$  in the absence of  $\text{Na}^+$  in the medium (35), and its pumping of either ion was shown to involve a BR-like outward displacement of helix 6 during the photocycle (39), indicating a close mechanistic relationship to rhodopsin proton pumps. Nearly all measurements of  $\text{Na}^+$  and  $\text{H}^+$  transport by NaRs have been conducted by recording passive and active light-driven proton fluxes, respectively, in live cell suspensions of the native organism or heterologously transformed *E. coli*. IaNaR, from *Indibacter alkaliphilus*, has been studied in a purified in vitro unilamellar vesicle system that demonstrated that the dual light-driven  $\text{H}^+/\text{Na}^+$  pumping functions are intrinsic to the single rhodopsin protein and provide a system in which ion flux measurements are not influenced by bioenergetic processes in living cells (38).

In the conserved NDQ motif of NaRs versus the DTD motif of BR, Asn112 in KR2 corresponds to D85 in BR, which is the retinylidene protonated Schiff base counterion and acceptor of the Schiff base proton in the BR pumping cycle. BR's Thr89 is not directly involved in proton transfer, but the corresponding residue Asp116 in KR2 has been shown to be the Schiff base proton acceptor (11). During the photocycle of BR, the proton transfers from the Schiff base to Asp85 on the extracellular side of the protein, and Schiff base reprotonates from Asp96, the third D in the DTD motif, from the cytoplasmic side, which causes vectorial translocation of the proton across the membrane. In contrast, a mechanism of flipping of the proton acceptor has been proposed for  $\text{Na}^+$  transport on the basis of a KR2 crystal structure (40). In the model, the ionized Asp116 serves as the Schiff base counterion and during the pumping cycle the protonated Asp116 flips away from the Schiff base, creating a space for  $\text{Na}^+$  during its transport through the protein. Reorientation of Asp116 toward the Schiff base was observed after soaking the crystal, obtained in acidic conditions, in alkaline conditions. In agreement, a simultaneously reported crystal structure in acidic conditions showed Asp116 oriented away from the Schiff base (41). A central role for



Asp116 was proposed from the original findings that the mutation D116N red-shifts the pigment 40 nm and blocks light-induced Schiff base deprotonation and ion pumping (35).

### Sensory Rhodopsins: Diverse Signaling Mechanisms

The first type 1 rhodopsin dedicated to sensory signaling rather than ion transport was discovered as a phototaxis receptor in *H. salinarum* in 1982, 10 years after the discovery of BR in the same organism. The light sensor, now known as sensory rhodopsin I (SRI), was followed by the finding of sensory rhodopsin II (SRII) in the same organism. Later, other sensory rhodopsins (channel-rhodopsins) were found to mediate phototaxis in the green alga *Chlamydomonas reinhardtii*, and a third form of type 1 rhodopsin, an enzymehhodopsin found in fungi, also appears to mediate phototaxis behavior. All of these sensory rhodopsins differ in their mechanisms of signaling to the motility apparatus of their host organism. Also a sensory rhodopsin implicated in regulation of gene expression was found in cyanobacteria, which also exhibits a different mode of signaling. Despite their differing signaling modes, sensory rhodopsins share features in their photochemical reaction cycles, including relatively stable states for signaling not found in rhodopsin ion pumps.

**Sensory rhodopsin/transducer complexes.** Light-modulated swimming behavior (phototaxis in the general sense of the term) is a well-known photosensory response among motile microorganisms. The first identified phototaxis receptor, which was also the first light-sensing receptor identified in a microorganism, was found in studies of *H. salinarum* photomotility responses (42, 43). Initially termed slow-cycling rhodopsin, the pigment is now known as SRI. SRI and SRII are subunits of membrane-embedded 2:2 complexes with cognate transducer proteins to which they transmit photosignals. Homologs of SR and transducer pairs were later found in other archaeons and in bacteria. A sensory rhodopsin from a cyanobacterium termed *Anabaena* sensory rhodopsin (ASR) binds to an unrelated cytoplasmic transducer.

**Sensory rhodopsin I.** The photochemical reactions of SRI (44) differed fundamentally from those of the other microbial rhodopsins known at the time, the ion pumps BR and HR. In the pumps, linear unbranched photochemical reaction cycles have been optimized by evolution to be rapid (~10 ms half time) with short-lived intermediates. In SRI a signaling conformer of the protein accumulates as a long-lived (~800 ms) spectrally shifted intermediate in a one-photon photochemical reaction cycle. The signaling conformer is photochemically reactive and is efficiently photoconverted back to the unphotolyzed (dark) state in ~70 ms by a second photon excitation of the molecule. This photochromic interplay of 1-photon formation and 2-photon reversion results in color-sensitive signaling that enables color-discriminating phototaxis by the organism (44). The single SRI molecule guides the cell toward higher intensities of long wavelength light useful for photoenergy capture by its light-driven pumps while also guiding the cell away from near-UV light, minimizing photooxidative damage. Relatively long-lived photoreversible signaling states are also a general property of sensory rhodopsins, discovered later. For example, channelrhodopsins exhibit a similar color-discriminating mechanism with similarly slow kinetics that enable the experimenter to control the lifetime of the spectrally shifted signaling conformer (the conductive state) by 1- and 2-photon excitation. The channelrhodopsins therefore can be used in optogenetics as bistable optical switches (45), photoactivated by one color of light and rapidly reset to the dark state by light of a different wavelength.

The methylated membrane protein HtrI (halobacterial transducer for SRI) was identified in the SRI signaling pathway by mutant analysis, and its gene cloned from a partial amino acid residue sequence obtained from the protein (46). The *htrI* gene was found to be immediately upstream of



*sopI* (sensory opsin I), which had been cloned previously. The genes encoding SRII and HtrII are similarly arranged, and the sensory rhodopsin/transducer complex (SR-Htr) bicistronic operons are also found in eubacteria. HtrI's very close homology to chemotaxis receptors (46), combined with behavioral effects of mutation of chemotaxis signaling components (47), led to the currently accepted signaling pathway from the receptors to the flagellar motor (9).

**Sensory rhodopsin II.** Takahashi and coworkers (48) proposed the existence of a second phototaxis receptor in *H. salinarum* on the basis of the action spectrum for repellent responses in highly aerobic conditions in which SRI (and BR) are produced at much lower levels. Spectroscopic and biochemical analyses identified the new pigment, which was simultaneously named phoborhodopsin (49) and SRII (50).

The first atomic structures of sensory rhodopsins—of SRII (51, 52), with a fragment of its Htr transducer (53), and later of ASR (54)—revealed that these sensory rhodopsins are built on the same scaffold as the light-driven proton pump BR with photoactive sites nearly identical to that of BR. SRI is capable of efficient but slow light-driven proton transport, but in its natural state its bound transducer HtrI inhibits its pumping activity (55). Transducer-free SRII is also capable of proton pumping (56). Structural changes caused by HtrII, its cognate transducer, binding to SRII have been identified by mutagenesis, vibrational spectroscopy, and motility behavior studies, after which the elucidation of the chemical requirements for signaling by SRII was sufficiently precise to enable mutagenic conversion of BR into a robust phototaxis receptor, signaling through the SRII transducer with 35% of native SRII efficiency (57).

Functional conversion by mutagenesis of BR into HR function (28), SRI into BR function (55), BR into SRII function (57), and recent studies of interconversions of ion specificity in eubacterial pumps (34, 58) have shed light at the atomic level on how natural selection has modified their common design to create the distinctly different consequences of their photoactivation. Interconversions illustrate that even small changes are capable of modifying existing protein scaffolds to create distinctly different protein chemistry, as recently discussed (59).

**Anabaena sensory rhodopsin: membrane-to-cytoplasm signaling.** The first sensory rhodopsin found in eubacteria (the cyanobacterium *Anabaena*, also known as *Nostoc*) was *Anabaena* sensory rhodopsin (ASR), so named due to its lack of pumping sequence motifs and its cotranscription from an operon with a soluble protein (later named ASR transducer, ASRT) that binds to it and alters its photoreactions (60). ASR exhibits photoreactions currently unique among type 1 rhodopsins in that illumination of its all-*trans* retinylidene chromophore form (with the position of the absorption maximum,  $\lambda_{\text{max}}$ , 550 nm for detergent-purified protein) produces a stable spectrally shifted 13-*cis*-retinal form ( $\lambda_{\text{max}}$  537 nm), the illumination of which reconverts to the all-*trans*-retinal form (54, 61). This type of photochromism is analogous to the well-known type in phytochromes. The physiological function of the ASR-ASRT pair is not fully elucidated. A study in *E. coli* showed that the ASR-ASRT complex could regulate expression of a reporter gene controlled by an *Anabaena* phycocyanine promoter (62). More recently, indicating physiological relevance of the *E. coli* study, biochemical and genetic evidence in *Anabaena* point to a role of ASRT in chromatic adaptation through regulated expression of genes encoding components of the phycobilin complex and a circadian clock gene (63). Specific reviews on ASR photochemical studies and physiological function are available (64, 65).

**Enzymerhodopsins: kinases and cyclases in algae and fungi.** The microbial rhodopsins discussed above are single-domain proteins. In both CCRs and ACRs, discussed in the next sections, the rhodopsin domain is linked to a bulky C-terminal extension in which no known functional

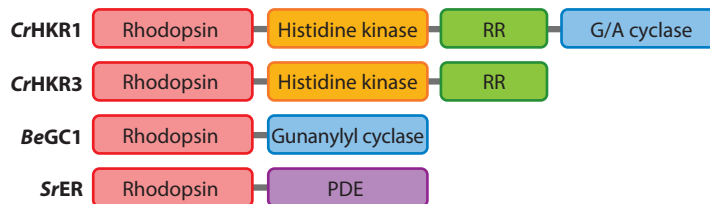


**Figure 3**

The domain structure of enzymerhodopsins. Abbreviations: *BeGC1*, rhodopsin guanylyl cyclase from the water mold *Blastocladiella emersonii*; *CrHKR1* and *CrHKR3*, histidine kinase rhodopsins 1 and 3, respectively, from the green alga *Chlamydomonas reinhardtii*; G/A cyclase, guanylyl/adenylyl cyclase domain; PDE, phosphodiesterase domain; RR, response regulator domain; *SrER*, enzymerhodopsin from the choanoflagellate *Salpingoeca rosetta*.

domains have been recognized. However, the genomes of some algae and fungi encode multidomain proteins, termed enzymerhodopsins, that comprise an N-terminal rhodopsin domain followed by domains found in proteins known to perform enzymatic functions. In proteins of this class a rhodopsin domain is linked to domains homologous to proteins of two-component signaling systems (histidine kinases and response regulators) and/or a guanylyl/adenylyl cyclase domain (**Figure 3**).

**Algal histidine kinase rhodopsins.** The first members of this class were identified in the genome of the green alga *C. reinhardtii* (66), which contains at least four such genes encoding histidine kinase rhodopsins (HKRs). HKR sequences have also been found in the genomes of several other algae (67).

HKR1 from *C. reinhardtii* is currently the only HKR, the rhodopsin domain of which has been heterologously expressed in *Pichia*, purified, and spectroscopically studied (68). It is a photochromic pigment with two forms, Rh-UV and Rh-BI, with absorption maxima at 380 nm and 490 nm, respectively, that are efficiently interconverted by light. In the dark, thermal equilibration of the two forms occurred with a time constant of  $\sim 3$  days at room temperature (69). Resonance Raman spectroscopy showed that Rh-UV contains 13-*cis*, 15-*anti* retinal bound to the apoprotein without forming a protonated Schiff base (68). Photoconversion from Rh-UV to Rh-BI proceeds in a branched reaction leading to two thermally interconvertible forms with protonated retinylidene Schiff bases containing 13-*trans*, 15-*anti* or 13-*cis*, 15-*syn* retinal. Rh-BI shows typical photochemistry as observed in other microbial rhodopsins. HKR1 fragments extending beyond the rhodopsin domain failed to fold properly in the heterologous systems tested (68), so HKR1's enzymatic function could not be studied. Immunofluorescent microscopy showed its localization in the eyespot of *C. reinhardtii* (68), but no rhodopsins aside from CCRs have been found in this organelle by proteomic analysis (70). Cellular functions of HKR1 are not known.

**Fungal guanylyl cyclase rhodopsins.** Motile zoospores and gametes of water molds such as *Allomyces macrogynus* and *Blastocladiella emersonii* exhibit phototaxis similar to those of green flagellate algae. The action spectrum of this response and its reconstitution after bleaching with exogenous retinal suggested a rhodopsin photoreceptor(s) (71, 72). The genomes of these microbes and their relative *Catenaria anguillulae* harbor genes that encode enzymerhodopsins consisting of a rhodopsin domain and a guanylyl cyclase domain (without histidine kinase or response regulator domains) (72). In contrast to all other type 1 rhodopsins, the rhodopsin domains of all five known fungal enzymerhodopsins (three from *A. macrogynus* and one each from *B. emersonii* and *C. anguillulae*) contain a predicted additional transmembrane helix in the N terminus (helix 0) (73). The

cytoplasmic localization of the N-terminal region has been confirmed by bimolecular fluorescence complementation, and its role in inhibition of the dark cyclase activity has been demonstrated by measurements from an N-terminally truncated version of the protein (73).

The results of pharmacological manipulation of the intracellular cGMP concentration and immunofluorescence microscopy in intact *B. emersonii* zoospores suggest the role of enzymerrhodopsin (*BeGC1*, rhodopsin guanylyl cyclase from *B. emersonii*) as a phototaxis receptor (72). It is thought that *BeGC1* initiates a signaling cascade that leads to the elevation of the intracellular cGMP concentration, which regulates opening of cGMP-gated K<sup>+</sup> channels identified in the genome of *B. emersonii* (74).

Unlike algal HKRs, the entire codon-optimized coding regions of fungal enzymerrhodopsins have been functionally expressed and studied in animal cells. *BeGC1* [under the names RhGC (75) and CyclOp (73)] produced the most robust elevation of the intracellular cGMP levels upon illumination of all tested homologous proteins, whereas its dark cyclase activity was very low and no intrinsic ion channel or pumping activity was detected (73, 75). High specificity of its cyclase domain for cGMP over cAMP (cyclic adenosine monophosphate) was demonstrated by coexpression with two different subtypes of the cyclic nucleotide-gated channel, each of which is specifically gated by one of the two cyclic nucleotides (75). Flash spectroscopy of the dark-adapted *BeGC1* ( $\lambda_{\text{max}}$  525 nm) produced at least three photocycle intermediates, including a blue-shifted M-like state characteristic of a deprotonated retinylidene Schiff base (75).

A third member of the enzymerrhodopsin class, a gene encoding a microbial rhodopsin domain followed by a phosphodiesterase (PDE) domain, has been found in the genome of the choanoflagellate *Salpingoeca rosetta* (72), but studies of its molecular characteristics have not yet been reported.

**Cation channelrhodopsins in green algae (chlorophyte CCRs).** Photoreceptors that guide phototaxis of green flagellates are so far the only eukaryotic microbial rhodopsin sensory functions that have been experimentally verified in native cells. The main reason for recently increased interest in these proteins is their use as optogenetic tools to depolarize the plasma membrane of excitable cells. Electrophysiological studies on chlorophyte CCRs in heterologous membranes under voltage clamp conditions have facilitated understanding of their conduction mechanisms, and investigation of detergent-purified proteins by optical and molecular spectroscopic methods have contributed to understanding of their structure-functional coupling.

**General properties and functions in native cells.** The photoinduction of electrical potentials involved in phototaxis was discovered by electrophysiological recording from algal cells (76). The first report regarding the chemical nature of the photoreceptors was the demonstration in 1984 that retinal restored phototaxis to carotenoid-deficient *C. reinhardtii* mutants (77). The number and molecular identity of the phototaxis receptor proteins remained elusive until two type 1 rhodopsins cloned from partial sequences in a *C. reinhardtii* expressed sequence tag database were each shown to mediate phototaxis responses by depolarizing the algal membrane upon illumination (78). When expressed in animal cells, the algal phototaxis receptors function as light-gated cation channels, for which they were named channelrhodopsins (ChR1 and ChR2) (79, 80). The use of *CrChR2* for photoinduction of action potentials in neurons (81) brought about the era of optogenetics (3, 4). Because the separate class of neuron-silencing ACRs has been recently discovered (82; see the next section), here we refer to cation channelrhodopsins as CCRs.

CCRs in green algae are the only group of eukaryotic microbial rhodopsins the physiological function of which in native cells is well characterized. Depolarization of the plasma membrane by CCRs triggers a signaling cascade that eventually leads to initiation of photomotility responses (83). The CCR-mediated photoreceptor current in algal cells comprises two components (84).

The fast (early) component is attributable to the later-shown direct channel activity of the CCRs. The slow (late) component is carried by  $\text{Ca}^{2+}$  ions and makes a major contribution to membrane depolarization, extending the photosensitivity of the algae by three orders of magnitude (85). RNAi knockdown experiments in *C. reinhardtii* demonstrated that both CCRs play the role of photophobic as well as phototaxis receptors (78, 86) and that short wavelength-absorbing *CrChR2* predominantly activates secondary  $\text{Ca}^{2+}$  channels by a yet-unknown mechanism (85).

More than 50 different natural CCRs from different chlorophyte species are known at present, but only a few of them have been investigated in detail (59, 87). Most mechanistic studies have been carried out using *CrChR2* as a prototype CCR and are summarized in recent excellent reviews (10, 88).

**The photoactive site and proton transfer reactions.** An X-ray crystal structure of a CCR chimera made of *CrChR1* and *CrChR2*, termed C1C2, shows that its photoactive site strongly resembles that of BR and *NpSR11* (89). It is generally accepted that in CCRs the photocycle initiated by the all-*trans* form leads to channel opening, but functional relevance of the photocycle of the 13-*cis* form is currently debated (90, 91). The ultrafast processes upon *CrChR2* photoexcitation have been reviewed elsewhere (10). In all currently studied CCRs, all-*trans* to 13-*cis* retinal isomerization is manifested by the formation of a red-shifted intermediate(s) (termed P500 according to the wavelength position of its absorption maximum in *CrChR2*) (92–94). Its decay leads to the appearance of an M-like intermediate (P390) blue-shifted by deprotonation of the Schiff base (95, 96). M formation proceeds in two kinetically distinct phases (93, 97, 98), suggesting the presence of two substates probably similar to M1 and M2 intermediates in the photocycle of BR.

Electrophysiological measurements of intramolecular proton transfers in *CaChR1* and *VcChR1* from *Chlamydomonas augustae* and *Volvox carteri*, respectively, showed that both active site carboxylates can serve as Schiff base proton acceptors (97). A novel two-step proton relay mechanism that transfers a proton from the Asp85 homolog to the Asp212 homolog during the primary photo-transition and from the Schiff base to the Asp85 homolog during M formation has been proposed for *CaChR1* on the basis of FTIR (Fourier transform infrared) difference spectroscopy (99). Intramolecular proton transfer currents are not detected by patch clamp recording from *CrChR2* and other high-efficiency CCRs, although an outward intramolecular proton transfer is observed in weaker CCRs such as *CaChR1* (97). The results from FTIR spectroscopy of *CrChR2* are somewhat conflicting. One study has concluded that only the Asp212 homolog serves as the Schiff base proton acceptor in this protein (98), whereas another has reported parallel protonation of both active site carboxylates simultaneously with Schiff base deprotonation, thus suggesting that both of these residues might act as proton acceptors in *CrChR2* also (100).

Conversion of the M intermediate to a red-shifted N/O species (P520) reflects reprotonation of the Schiff base (95, 96). Time-resolved FTIR spectroscopy has identified Asp156 (corresponding to Asp115 in BR; **Figure 4a**) as the proton donor in *CrChR2* (98, 101). However, this conclusion has been challenged by the observation that the kinetics of Asp156 deprotonation do not match the Schiff base reprotonation (88). FTIR spectroscopy suggested a hydrogen-bonding interaction between Asp156 and Cys128 (Thr90 in BR), the so-named DC gate (102) disruption of which results in a dramatic reduction of the channel closing rate (103).

Flash photolysis reveals complexity due to branching within CCR photocycles. In both *CrChR2* (98) and *PcChR2* (94), P520 decays in ~10 ms but only ~75% of the molecules return to the unphotolyzed state, whereas the remaining 25–30% convert to the seconds-lifetime P480. Furthermore, analysis of photochemical conversions in the slow *CrChR2\_C128T* mutant has suggested the existence of two stable unphotolyzed states, one of which contains all-*trans*, 15-*anti* retinal, and another, 13-*cis*, 15-*syn* retinal (104). These forms have been modeled as the parent states of two

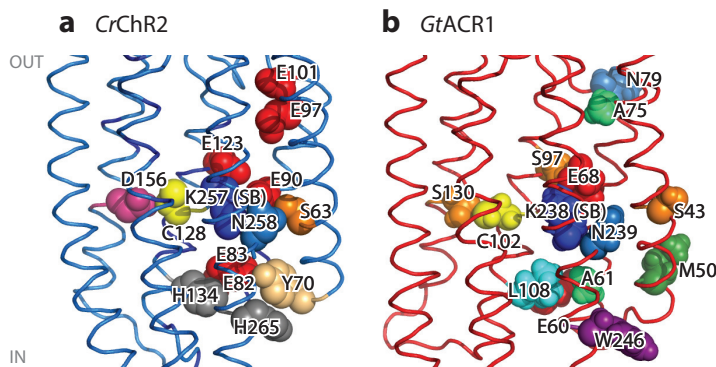


**Figure 4**

Functionally important residues in chlorophyte CCRs and cryptophyte ACRs. (a) Crystal structure (3ug9) of C1C2, a CCR chimera made of transmembrane helices 1–5 of CrChR1 and helices 6–7 of CrChR2 with residues numbered according to CrChR2 sequence. (b) GtACR1 homology model built using 3ug9 as a template. The side chains are colored according to their identity. Abbreviations: ACRs, anion channelrhodopsins; CCRs, cation channelrhodopsins; CrChR1 and 2, channelrhodopsins 1 and 2 from *Chlamydomonas reinhardtii*; GtACR1, ACR1 from *Guillardia theta*.

parallel photocycles, each of which contains P390, P520, and P480 intermediates, with the two photocycles linked by interconversion of the long-lived P480 states. This scheme has also been extended to the wild type, for which a two-photocycle model was deduced earlier from electrophysiological data with the difference that the two cycles are connected via unphotolyzed states, not long-lived P480 states (105). The latter scheme was also suggested by a combination of flash photolysis, nuclear magnetic resonance, and resonance Raman spectroscopy data (90).

**Channel gating.** The C1C2 crystal structure of the closed state shows that helices 1–3 and 7 form a water-filled cavity at the extracellular side of the membrane (89). This cavity is blocked near the Schiff base by the so-named central gate formed by the side chains of Ser63, Glu90, and Gln258 (CrChR2 numbering; **Figure 4a**). There is also a constriction (termed the inner gate) near the intracellular membrane surface formed by the side chains of Tyr70, Glu82, Glu83, His134, and His265 (CrChR2 numbering; **Figure 4a**). Large conformational changes in the peptide backbone occur rapidly upon retinal isomerization (106, 107). Double electron–electron resonance (DEER) spectroscopy indicated that the intracellular end of helix 2, and of helix 6 to a lesser degree, move outward upon illumination (108, 109). The results of time-resolved measurements of fluorescence anisotropy are consistent with an outward tilt of helix 2 (110). Projection maps obtained by cryo–electron microscopy additionally suggested a photoinduced movement of helix 7 (111). The outward movement of helix 6 (accompanied in BR by more subtle rearrangements of the cytoplasmic portions of helices 3, 5, and 7) is the major conformational change that occurs during the M1→M2 transition in BR (112), NaR (39), SRI (113), and SRII (113, 114). However, structural rearrangement of helix 2 appears to be unique for CCRs and is thought to play a major role in formation of a conducting pore (100).

P520 is generally accepted as the main conductive state, whereas contribution of P390 (corresponding to BR’s M), which is in equilibrium with P520, has also been implicated (103). Time-resolved FTIR analysis has shown that water influx upon photoactivation proceeds in two temporally separated steps with time constants of 10 and 200  $\mu$ s (115).

Photocurrents of all currently studied CCRs exhibit inactivation (also termed desensitization; i.e., a decrease in the photocurrent amplitude to a stationary level during prolonged light



stimulation). Inactivation is explained by accumulation of the long-lived nonconductive state(s) P480 (95, 96). A slow (tens of seconds) time course of the photocurrent peak recovery in the dark reflects slow relaxation of P480 to the unphotolyzed state. The central gate Glu90 deprotonates during the photocycle and, according to one view, this event initiates formation of the conductive pore (100, 116). However, other authors have proposed that deprotonation of Glu90 occurs only during the formation of the nonconductive P480 intermediate (98, 101).

**Conductance and selectivity.** Stationary noise analysis has yielded the value of 40 femtosiemens as an estimate of the unitary conductance of *CrChR2* (117), and an ~3-fold greater value was obtained for *PsChR2* from *Platymononas (Tetraselmis) subcordiformis* (118). All currently tested CCRs are primarily  $H^+$  channels: Their relative permeability for this ion is ~6 orders of magnitude greater than that for monovalent metal cations (80). The  $Na^+/H^+$  permeability ratio is, nevertheless, different for different ChRs (59). Regardless, under physiological conditions a large fraction of CCR current is carried by  $Na^+$  because the concentration of  $Na^+$  in physiological solutions is several orders of magnitude higher than that of  $H^+$  (119).

**Utility for optogenetics.** CCRs are widely used to depolarize the membrane and stimulate action potential generation in excitable cells and, less frequently, to alter the intracellular ionic composition. Many excellent reviews cover this topic in detail (3, 4, 120, 121); therefore, we touch upon it only briefly. Despite the great variety of available CCRs, *CrChR2* and its derivatives, such as *CrChR2\_H134R*, remain the most frequently used activation molecules in optogenetic experiments (122). Extensive engineering efforts have yielded synthetic variants with red- (123) or blue-shifted absorbance (124), altered current kinetics (45), or increased relative permeability for individual cation species (125). Moreover, by introducing strategically placed mutations, CCRs have been converted into light-gated  $Cl^-$  channels (discussed in the next section). Systematic comparative analyses of the optogenetic utility of various natural and artificial CCRs have provided the guidelines for selection of optimal tools for a particular experimental purpose (126–128).

A promising direction to improve the penetration depth of optical stimulation is two-photon excitation of CCRs with near-infrared light (129). Promising strategies are being developed for specific targeting of CCRs to subcellular domains (130), combining two spectrally separated CCRs for independent optical stimulation of distinct neuronal populations in the same study (87), and using a CCR as an actuator and an engineered fluorescent microbial rhodopsin as a reporter to achieve powerful all-optical recording of neuronal activity (131).

**Anion channelrhodopsins: natural chloride channels in cryptophyte algae.** In addition to green flagellates, the ability to track light direction was also observed in cryptophyte algae, so their genomes seemed likely to harbor genes encoding channelrhodopsin-like proteins. However, the closest structural homologs of chlorophyte CCRs found in cryptophytes turned out to be light-gated anion channels (ACRs), previously unknown to exist in nature. These proteins generate large hyperpolarizing photocurrents at membrane potentials above the Nernst equilibrium potential for  $Cl^-$  and can be used to suppress neuronal spiking at light intensities far lower than those required by other currently known inhibitory optogenetic tools.

**Conductance and diversity.** Photocurrents very similar to those in green flagellates have also been recorded from the phylogenetically distant phototactic cryptophyte *Cryptomonas* sp. (132). The only cryptophyte with a completely sequenced genome is the marine alga *Guillardia theta*. Among 53 predicted microbial-type rhodopsins in this organism, a cluster shows closer homology to chlorophyte CCRs than to other *G. theta* rhodopsins. Surprisingly, photocurrents generated

by these rhodopsins upon expression in animal cells were carried exclusively by anions ( $\text{Cl}^-$  under physiological conditions), with no conduction of protons or metal cations (82). Therefore, these proteins were termed anion channelrhodopsins (ACRs).

The unitary conductance of *Gt*ACRs estimated by stationary noise analysis was ~25-fold greater than that of *Cr*ChR2 (82). The spectral sensitivities of *Gt*ACR1 and *Gt*ACR2 photocurrents peak at 515 and 470 nm, respectively. Another cryptophyte alga, *Proteomonas sulcata*, contained a channelrhodopsin initially named *Ps*ChR1 (87), which was renamed *Psu*ACR1 (also known as *Ps*ACR1) when shown to exclusively conduct anions (133, 134). Screening sequences obtained by ongoing transcriptome sequencing projects (135, 136) expanded the list of functional ACRs to include 20 proteins derived from various marine cryptophyte species. These proteins showed large variation in the amplitude, spectral sensitivity, and kinetics of their photocurrents (162). One variant, ZipACR, is particularly promising for inhibitory optogenetics because of its combination of large current amplitudes and an unprecedentedly fast conductance cycle (current half-decay time is 2–4 ms depending on voltage). ZipACR expressed in cultured rat hippocampal neurons enabled precise photoinhibition of individual spikes in trains of up to 50 Hz frequency (162). Neither subcellular localization nor functions of ACRs in algal cells have yet been tested.

**Residue determinants of anion selectivity.** A conspicuous feature of ACRs is a noncarboxylic residue in the position of the primary proton acceptor from the retinylidene Schiff base of BR (Asp85; **Figure 4b**), as is also observed in haloarchaeal HRs and chloride pumps from eubacteria. In *Gt*ACR1, replacement of the corresponding Ser with Glu (found at this site in most CCRs) led to a dramatic reduction of the current amplitude in response to the first excitation flash, suggesting a critical importance of a noncarboxylate residue at this position for ACR channel function (137). However, the lack of a carboxylate residue in this position itself does not confer anion selectivity: For example, ChR1 from *Dunaliella salina* (*Ds*ChR1) has an Ala but is a proton channel (138).

Glu90 and Asn258 of the central gate in CCRs are also conserved in all currently confirmed ACRs, and the position of Ser63 is occupied by Ser or Cys (**Figure 4b**). Glu90 is a major determinant of cation selectivity in CCRs (116, 139). However, the presence of Glu in the corresponding position in ACRs (**Figure 5**) is obviously not a barrier to anion permeation, and its replacement with Gln or Arg does not change anion selectivity of *Gt*ACR1 (140). Therefore, the Ser, Glu, Asn triad does not appear to function as an ion-selective gate in ACRs.

In contrast to the central gate residues, only one of the five residues that form the inner gate in CCRs (Glu82) is found in all ACRs, but none of the other four (Tyr70, Glu83, His134, and His265) is conserved (**Figure 4b**). Whereas replacement of Glu82 with Ala caused a strong reduction of photocurrents in *Cr*ChR2, the influence of the corresponding mutation in *Gt*ACR1 was much milder (140), which suggests that this conserved residue also plays different roles in ACRs and CCRs, as does the homolog of Glu90.

**Sequence comparison with engineered  $\text{Cl}^-$ -conducting mutants of CCRs.** A need for more efficient inhibitory optogenetic tools than rhodopsin proton and chloride pumps instigated molecular engineering efforts to confer anion conductance to CCRs. One variant named ChloC was created by introducing an Arg at the position of the central gate Glu (the E90R mutation) in *Cr*ChR2 (139). Although permeant for  $\text{Cl}^-$ , ChloC also conducted protons, but its  $\text{H}^+$  permeability could be eliminated by introducing two additional mutations (141). The second variant (iC1C2) was created by introducing nine mutations along the putative cation permeation path of C1C2 to minimize its negative charge (142). This version also showed residual  $\text{H}^+$  permeability, but further mutations resulted in iC<sup>++</sup> that could track  $\text{Cl}^-$  gradients more faithfully (143).

Although engineering of anion conductance in CCRs was a notable achievement that confirmed fundamental predictions of a structure-informed electrostatic model for CCR pore selectivity,



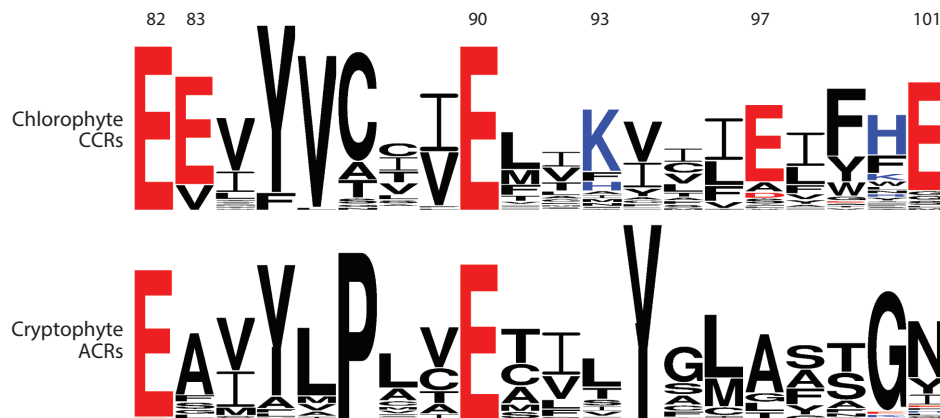


**Figure 5**

Helix 2 sequence logos of chlorophyte CCRs and cryptophyte ACRs created using WebLogo 3 as described in Reference 153. The overall height of each letter stack is proportional to the sequence conservation at that position, and the height of each letter is proportional to the frequency of the corresponding amino acid residue at that position. Acidic residues are red, and basic residues are blue. The numbers on top are those of the residues according to the *CrChR2* sequence. Abbreviations: ACRs, anion channelrhodopsins; CCRs, cation channelrhodopsins; *CrChR2*, channelrhodopsin 2 from *Chlamydomonas reinhardtii*.

comparison of the mutations introduced in CCRs to convert them into  $\text{Cl}^-$ -conducting channels with the corresponding positions in natural ACRs reveals dramatic differences. The most informative difference is universal conservation of Glu90 (*CrChR2* numbering) in natural ACRs, whereas in all engineered  $\text{Cl}^-$ -conducting CCR variants this Glu needed to be replaced with a neutral or even positively charged residue. Furthermore, out of two positions at which positive charges were introduced in  $\text{iC}^{++}$ , one (Gln117 in *CrChR2*) is occupied with a neutral residue and another (Val242 in *CrChR2*) with a negatively charged residue in all natural ACRs. These mismatches show that, unlike artificial  $\text{Cl}^-$ -conducting mutants, natural ACRs are not CCRs with just a few mutations conferring anion selectivity (144) but are a truly distinct family of channelrhodopsins (Figure 6).

**Gating mechanisms.** Kinetic analysis of photocurrents generated by *GtACR1* under single turnover conditions revealed that its conductance comprises two different mechanisms, one characterized by a fast rise and slow decay of photocurrents and another with a slow rise and fast decay (140). The two mechanisms of *GtACR1* gating exhibited opposite dependencies on the membrane voltage and the bath pH. Mutant screening revealed that deprotonation of Glu68, the homolog of Glu90 in *CrChR2*, to the extracellular side of the membrane is involved in fast closing of the channel.

Remarkably, when a positive charge was introduced at this site by the E68R mutation, channel gating was reversed (i.e., the channel was open in the dark and closed in the light) (140). No such form of a channelrhodopsin had been reported previously, but a similar functional inversion (from attractant to repellent signaling) by a single point mutation either of the photoreceptor itself or of its cognate transducer has been observed in haloarchaeal SRI (145–149). In this case, a switch from the C (retinylidene Schiff base accessible from the cytoplasm) to E (Schiff base accessible from the extracellular space) conformer is responsible for the functional inversion. Similarly, the inverted function of *GtACR1*\_E68R is likely to result from a mutation-induced inversion of its slow opening/fast closing gate.

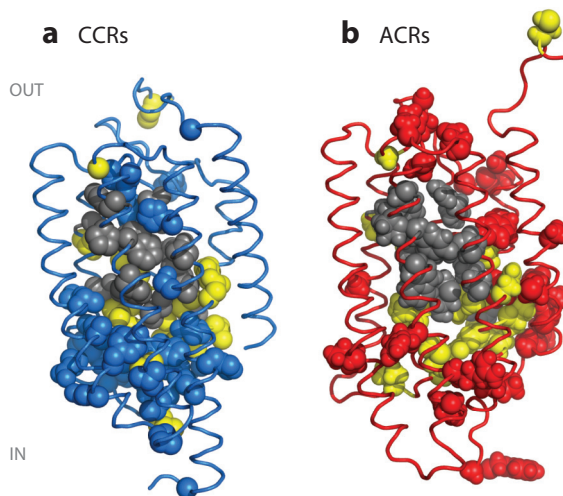


**Figure 6**

Structural comparison of chlorophyte CCRs and cryptophyte ACRs. Residues of the retinal binding pocket of bacteriorhodopsin conserved in each of the two types of channelrhodopsins (*gray*), residues conserved in both CCRs and ACRs (*yellow*), residues conserved only in CCRs (*blue*), and residues conserved only in ACRs (*red*) are shown. The residue conservation pattern is shown using (*a*) the C1C2 crystal structure (3ug9) and (*b*) a *GtACR1* homology model built on the 3ug9 template. Abbreviations: ACRs, anion channelrhodopsins; C1C2, a hybrid CCR made from channelrhodopsin 1 and channelrhodopsin 2 of *Chlamydomonas reinhardtii*; CCRs, cation channelrhodopsins; *GtACR1*, ACR1 from *Guillardia theta*.

Replacement of Cys102 with Ala in *GtACR1* has very little effect on the fast phase of the current decay but dramatically slows the slow phase, converting *GtACR1* into a step-function channel (140). Cys102 of *GtACR1* corresponds to Cys128 of *CrChR2*, the mutation of which leads to a similarly large decrease of the current decay rate (45). In *CrChR2* the C128X mutations presumably cause a disruption of the hydrogen bond (DC-gate) that Cys128 is proposed to form with Asp156 (102); this explanation is supported by the observation that mutation of Asp156 yielded comparable or even greater extension of the channel open time, as did that of Cys128 (103). However, in contrast to *CrChR2*, mutation of Ser130, which in *GtACR1* corresponds in position to Asp156, has little effect on the current decay rate, which suggests that the effect of the C102A mutation in *GtACR1* is not caused by disruption of a putative hydrogen bond (140).

**Photochemical conversions.** Photoactive *GtACR1*, *GtACR2*, and *PsuACR1* could be produced in *Pichia*, extracted in nondenaturing detergent, and studied in vitro. A resonance Raman study of *GtACR1* showed that the retinal chromophore exists in an all-*trans* configuration with a protonated Schiff base very similar to that of BR (150). The most striking difference between the photocycle of all three currently tested ACRs and other type 1 rhodopsins is an extremely slow appearance and decay of a blue-shifted M-like intermediate with a deprotonated retinylidene Schiff base (134, 137). In CCRs, M formation occurs within microseconds to tens of microseconds and precedes channel opening (92, 96, 97). In contrast, M formation in *GtACR1* is >50 times slower than channel opening, showing that the latter does not require Schiff base deprotonation.

In ACRs the open state is represented by the earlier L-like intermediate that appears on a sub-millisecond timescale and decays to form M, although a rapid equilibrium between the L and an open-state red-shifted N/O-like intermediates cannot be excluded. Channel closing correlates

with formation of M. The fast phase of channel closing temporally corresponds to the depletion of the L state and consequent generation of M because of the rapid reversible equilibrium between the L and M intermediates, whereas slow channel closing corresponds to the irreversible decay of M (and, hence, of L). When Cys102 was mutated to Ala in *GtACR1*, both M decay and recovery of the unphotolyzed state became ~100-fold slower than in the wild type (137), which matched the influence of this mutation on the slow phase of the photocurrent decay.

In HRs, which have a noncarboxylate residue in the position of Asp85 of BR as do ACRs, Cl<sup>-</sup> acts as the protonated Schiff base counterion (151). However, deionization of purified pigment or substitution of SO<sub>4</sub><sup>2-</sup> for Cl<sup>-</sup> in the buffer changed neither the position of the absorption maximum nor the photocycle of *GtACR1*, which argues against Cl<sup>-</sup> being a Schiff base counterion in this rhodopsin (137). Patch clamp and flash photolysis analysis of the *GtACR1\_E68Q* mutant suggests that Glu68 likely serves as a counterion and an acceptor of the proton from the Schiff base at neutral and high pH, or at least facilitates the proton transfer to the acceptor (137). Resonance Raman spectroscopy data are not consistent with this residue acting as a Schiff base counterion at neutral pH, but it cannot be excluded that Glu68 deprotonates early in the photocycle and accepts a proton from the Schiff base during formation of the M intermediate (150). A similar two-step process has been shown by resonance Raman and FTIR-difference spectroscopy for the Asp85 homolog in the cation channelrhodopsin *CaChR1* (99). The role of Glu68 as a proton acceptor in *GtACR1* is supported by the Glu68 dependence of an outward proton transfer current evident in a mutant in which the second photoactive site carboxylate, Asp234, is neutralized (137).

**Utility for optogenetics.** As of this writing, the most frequently used inhibitory optogenetic tools are rhodopsin proton and chloride pumps such as Arch (14) and *NpHR* (29). However, they transport only one charge across the membrane per captured photon and therefore are of limited capacity. Their use as optogenetic silencing tools requires high expression levels and light intensities, which can bring about undesired side effects on the health of target cells. In contrast, ACRs (as well as Cl<sup>-</sup>-conducting CCR mutants) facilitate ion passage along a water-filled cavity that is formed within the protein upon photoexcitation and thus are intrinsically more efficient than rhodopsin ion pumps. Furthermore, they bring the membrane potential to the Nernst equilibrium potential for Cl<sup>-</sup>, as do endogenous neuronal ionotropic gamma-aminobutyric acid receptors, and in this sense are more physiological silencing tools than rhodopsin pumps.

Hyperpolarizing photocurrents generated by *GtACR2* at less than a thousandth lower light intensity were equal to the maximal currents generated by Arch or slow ChloC (82). Robust inhibition of action potential firing has been demonstrated in cultured hippocampal neurons expressing *GtACR2* (82) and *GtACR1*-expressing neurons (152). Expression of either *GtACR1* or *GtACR2* in *Drosophila* neurons enabled temporally precise silencing of spikes and inhibition of a wide range of behavioral and physiological responses in live animals (locomotion, wing expansion, memory retrieval, and gustation) (153).

However, photoactivation of *GtACR1* triggered neurotransmitter release and failed to attenuate the evoked response at the presynaptic terminals in cultured rat hippocampal neurons (152), consistent with the finding that the Cl<sup>-</sup> concentration maintained in the axon terminals is four to five times higher than that in the parent cell soma. Therefore, for inhibition of synaptic release, ACRs will need to be targeted exclusively to somatodendritic membrane domains. Alternatively, outwardly rectifying ACR variants need to be engineered to prevent Cl<sup>-</sup> efflux at membrane potentials below the Nernst equilibrium potential for Cl<sup>-</sup>.

Optogenetic applications of ACRs are not limited to hyperpolarization of the membrane. In combination with the hyperpolarizing proton pump ArchT, *GtACR2* as well as an engineered

$\text{Cl}^-$ -conducting CCR mutant have been used to reduce the intracellular  $\text{Cl}^-$  concentration by promoting  $\text{Cl}^-$  extrusion from neurons (154). Dynamic changes in the  $\text{Cl}^-$  level have been implicated in many aspects of neuronal physiology and pathophysiology. In particular, elevated neuronal  $\text{Cl}^-$  loads are associated with epilepsy, and the emerging possibility of their optogenetic correction paves the way to new treatments of this disorder.

Another research area in which ACRs may find application as optogenetic tools is cardiology. Whereas cardiac pacing by light requires membrane-depolarizing, excitatory optogenetics tools, optogenetic inhibition is needed to study diseases of the heart conduction system or tachyarrhythmias. *Gt*ACRs have been found more efficient than Arch for silencing of electrical activity in cultured cardiomyocytes (155). Moreover, *Gt*ACRs enabled precise termination of cardiomyocyte action potentials at any time during their repolarization phase by threshold-based closed-loop optogenetics, which can potentially be used for the development of new treatments for the life-threatening long QT syndrome (155).

### Cryptophyte CCRs: independently evolved cation channels from haloarchaeal ancestors.

A distinct branch on the phylogenetic tree of *G. theta* rhodopsins consists of nine protein models, the closest homologs of which in the global nonredundant protein database are haloarchaeal rhodopsin proton pumps (156). In particular, Asp residues in the positions of the Schiff base proton acceptor and donor (respectively, Asp85 and Asp96 in BR) are conserved (Figure 7). The presence of these carboxylates in microbial rhodopsins in general is considered a strong indicator of proton pumping ability, although counterexamples have been described, such as a rhodopsin

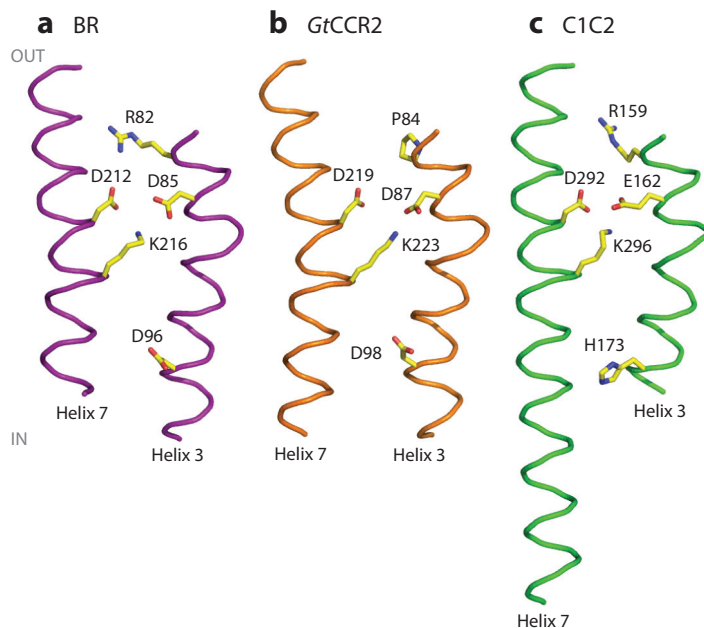


**Figure 7**

The active site residues of cryptophyte CCRs. (b) A *Gt*CCR2 homology model built on the 2ksy template in comparison with (a) those of the proton pump BR (1c3w) and (c) chlorophyte CCR C1C2 (3ug9). For clarity only helices 3 and 7 are shown. Abbreviations: ACRs, anion channelrhodopsins; BR, bacteriorhodopsin; CCRs, cation channelrhodopsins; C1C2, a hybrid CCR made from channelrhodopsin 1 and channelrhodopsin 2 of *Chlamydomonas reinhardtii*; *Gt*ACR1, ACR1 from *Guillardia theta*.

from the fungus *Neurospora crassa* (157). Despite their similarity of sequence to light-driven proton pumps, when three transcripts from this *G. theta* cluster and a close homolog from *P. sulcata* were expressed in cultured animal cells, they behaved as light-gated cation channels (156).

As discussed in previous sections, helix 2 is critically important for channel gating in chlorophyte CCRs. Helix 2 contains up to five highly conserved Glu residues, one of which, Glu90 in *CrChR2*, plays a crucial role in both channel gating and cation selectivity (100, 139). However, none of these Glu residues are conserved in cryptophyte CCRs, and their overall helix 2 sequence is highly divergent from that of CCRs from green algae.

Two unusual representatives of this group are two *G. theta* CCRs in which homologs of Arg82 (BR numbering), nearly universally conserved in microbial rhodopsins, are substituted by Pro. Functional characteristics of *GtCCR1* and *GtCCR2* are very different from other characterized CCRs. Two processes contribute to the photocurrents generated by these pigments: (a) sodium channel conductance with strong inward rectification of the current-voltage dependence and (b) active outward proton transfer, which exhibits a large negative reversal potential and is strongly suppressed by an increase in the external proton concentration (O.A. Sineshchekov, E.G. Govorunova, H. Li, and J.L. Spudich, manuscript in preparation).

The Schiff base donor position in cryptophyte CCRs is occupied by Asp, instead of His as in chlorophyte CCRs. Neutralization of this residue caused full suppression of passive channel activity, demonstrating another crucial difference between the two families of CCRs (O.A. Sineshchekov, E.G. Govorunova, and J.L. Spudich, manuscript in preparation).

The cryptophyte CCRs reveal that cation channel function can be conferred on the rhodopsin scaffold in structurally different ways. These proteins have not yet been characterized in detail, but their identification has already shown that our current view of channelrhodopsins needs to be updated. At least one of the four currently examined cryptophyte CCRs generated photocurrents comparable to those of chlorophyte *CrChR2*, the most often used optogenetic tool (156). The ongoing transcriptome sequencing projects (135, 136) have uncovered >60 of their homologs in various cryptophyte species. Some of them may have even higher conductance like their ACR cousins and offer advantages for optogenetic neural activation.

## FUTURE PROSPECTS IN RESEARCH AND CLINICAL OPTOGENETICS

The surprising discovery in the past 2 years of three structurally and functionally distinct families of channelrhodopsins, when only one family, chlorophyte CCRs, had been known for the prior 15 years, has expanded research opportunities and enabled some prior limitations to structure/function analysis of channel mechanism to be overcome. It is evident from the early investigations of the two new classes of channelrhodopsins, ACRs and cryptophyte CCRs, that their selectivity, conductance, and gating mechanisms differ greatly from those of chlorophyte CCRs. Hence their elucidation along with further advances on chlorophyte CCRs are likely to give us a deep understanding of light-gated channel function and evolution. Natural ACRs offer two clear advantages for channelrhodopsin research. First, one of the main limitations to the study of chlorophyte CCRs has been their relatively low conductance, and ACRs are the most conductive light-gated channels known, providing a practical advantage for structure/function analysis. Second, the availability of an inverted ACR mutant, *GtACR1\_E68R*, open in the dark and closed by illumination, provides a valuable complement to the wild-type ACR for structure/function analysis. X-ray crystal structures of both would be fascinating to compare and are almost certainly necessary for an atomic understanding of the gating mechanism.

Light-gated channel activity of purified *GtACR1* incorporated in large unilamellar vesicles was assessed by measurements of pH changes due to secondary  $H^+$  fluxes, which demonstrated

that this protein retained functionality in synthetic membranes (158). The purified system allows measurement of channel photocurrents and is amenable to optical and molecular spectroscopic probes of structural changes. With high time-resolution membrane-embedded voltage sensors, this system may enable more direct investigation of the coupling between structural changes and channel gating.

The cryptophyte CCRs have converged on cation channel function via a different evolutionary route than their distant chlorophyte cousins. Therefore, the mechanistic features shared by these two very different cation channels will help us understand the core requirements for light-gated cation conductance.

The physiological function of the cryptophyte channelrhodopsins, and of the large variety of other type 1 rhodopsins found in individual cryptophyte genomes, remains mysterious. The spectral sensitivity of photomotility responses in cryptophyte algae is consistent with the spectral range of rhodopsin absorption (132, 159), but given the large number of rhodopsin genes in individual cryptophyte genomes, probing the cellular roles of rhodopsins, including ACRs in cryptophyte algae, will require the development of methods for their molecular genetic manipulation, similar to those used in *C. reinhardtii* (78).

In addition to the mystery of light-gated anion channel conductance as a previously unknown phenomenon in nature, ACRs have generated much interest as optogenetic tools because of their unprecedented photoefficiency to silence neurons by light-gated chloride conduction. As discussed above, owing to their potency and the variation in the  $\text{Cl}^-$  electrochemical potential in neurons, work on targeting ACRs to neuronal compartments and engineering of outwardly rectified variants would be useful to expand their utility as optogenetic tools. Cryptophyte CCRs, in an early stage of investigation, also may offer new properties for optogenetic use based on their different origins. Enzymerhodopsins, also little studied, are expected to provide new ways to use light for control of cell signaling and metabolism, expanding optogenetics with microbial rhodopsins beyond control of membrane electrical potential.

Clinical optogenetics is in its infancy but can be expected to grow rapidly given its advantages for gene therapy. Optogenetics enables control of genetically targeted populations of neurons without affecting other neurons. Therefore optogenetic gene therapy provides a more precise and less invasive strategy for neuromodulation than pharmaceuticals or electrical implants. The most developed potential therapeutic application of optogenetics is the use of CCRs to restore vision in retinal degenerative diseases. In several such diseases (hereditary retinitis pigmentosa, diabetic retinopathy, and age-related macular degeneration) blindness results from death of the photoreceptor neurons (rods and cones) (160). The strategy is to express a neuron-activating CCR in downstream retinal neurons to confer photosensitivity to these components of the visual pathway, bypassing the missing or degenerated rods and cones. Animal studies have proven promising (161), and the first human clinical trials to test gene therapy with *CrChR2* for vision restoration to blind retinitis pigmentosa patients began this past year (ClinicalTrials.gov Identifier: NCT02556736). The combination of inhibitor and activator optogenetic tools may enhance this therapeutic approach since human vision entails an interplay of photoinhibition and photoactivation of neural pathways, especially in cone-mediated visual transduction.

Clinical optogenetics necessarily began with a neuron-activating CCR because efficient neuron inhibitors were not available. The discovery of ACRs opens the way for similar gene therapy for conditions in which excessive neural firing is involved. Indeed, neuron hyperactivity is centrally involved either as a cause or as a major symptom in myriad neurological disorders, such as epilepsy, Parkinson's disease, autism, tinnitus, migraine, and chronic and post-operative neuropathic pain.



## DISCLOSURE STATEMENT

J.L.S., E.G.G., and O.A.S. are listed as inventors on patent applications regarding channel-rhodopsins filed by The University of Texas Health Science Center at Houston.

## ACKNOWLEDGMENTS

J.L.S. acknowledges financial support from the National Institutes of Health (NIH) National Institute of General Medical Sciences, the NIH BRAIN Initiative, and endowed chair AU-0009 from the Robert A. Welch Foundation.

## LITERATURE CITED

1. Spudich JL, Yang C-S, Jung K-H, Spudich EN. 2000. Retinylidene proteins: structures and functions from archaea to humans. *Annu. Rev. Cell Dev. Biol.* 16:365–92
2. Devine EL, Oprian DD, Theobald DL. 2013. Relocating the active-site lysine in rhodopsin and implications for evolution of retinylidene proteins. *PNAS* 110:13351–55
3. Boyden ES. 2015. Optogenetics and the future of neuroscience. *Nat. Neurosci.* 18:1200–1
4. Deisseroth K. 2015. Optogenetics: 10 years of microbial opsins in neuroscience. *Nat. Neurosci.* 18:1213–25
5. Ernst OP, Lodowski DT, Elstner M, Hegemann P, Brown LS, Kandori H. 2014. Microbial and animal rhodopsins: structures, functions, and molecular mechanisms. *Cchem. Rev.* 114:126–63
6. Essen LO. 2002. Halorhodopsin: Light-driven ion pumping made simple? *Curr. Opin. Struct. Biol.* 12:516–22
7. Lanyi JK. 2006. Proton transfers in the bacteriorhodopsin photocycle. *Biochim. Biophys. Acta* 1757:1012–18
8. Balashov SP, Lanyi JK. 2007. Xanthorhodopsin: proton pump with a carotenoid antenna. *Cell. Mol. Life Sci.* 64:2323–28
9. Spudich JL, Spudich EN. 2008. The simplest eyes: rhodopsin-mediated phototaxis reception in microorganisms. In *Animal Models in Eye Research*, ed. PA Tsonis, pp. 6–14. Amsterdam: Elsevier
10. Lorenz-Fonfria VA, Heberle J. 2014. Channelrhodopsin unchained: structure and mechanism of a light-gated cation channel. *Biochim. Biophys. Acta* 1837:626–42
11. Inoue K, Kato Y, Kandori H. 2015. Light-driven ion-translocating rhodopsins in marine bacteria. *Trends Microbiol.* 23:91–98
12. Oesterhelt D, Stoekenius W. 1971. Rhodopsin-like protein from the purple membrane of *Halobacterium halobium*. *Nature* 233:149–52
13. Henderson R, Unwin P. 1975. Three-dimensional model of purple membrane obtained by electron microscopy. *Nature* 257:28–32
14. Chow BY, Han X, Dobry AS, Qian X, Chuong AS, et al. 2010. High-performance genetically targetable optical neural silencing by light-driven proton pumps. *Nature* 463:98–102
15. Beja O, Aravind L, Koonin EV, Suzuki MT, Hadd A, et al. 2000. Bacterial rhodopsin: evidence for a new type of phototrophy in the sea. *Science* 289:1902–6
16. Beja O, Spudich EN, Spudich JL, Leclerc M, DeLong EF. 2001. Proteorhodopsin phototrophy in the ocean. *Nature* 411:786–89
17. Venter JC, Remington K, Heidelberg JF, Halpern AL, Rusch D, et al. 2004. Environmental genome shotgun sequencing of the Sargasso Sea. *Science* 304:66–74
18. Sabehi G, Loy A, Jung KH, Partha R, Spudich JL, et al. 2005. New insights into metabolic properties of marine bacteria encoding proteorhodopsins. *PLOS Biol.* 3:e273
19. Ran T, Ozorowski G, Gao Y, Sineshchikov OA, Wang W, et al. 2013. Cross-protomer interaction with the photoactive site in oligomeric proteorhodopsin complexes. *Acta Crystallogr. Sect. D* 69:1965–80
20. Hussain S, Kinnebrew M, Schonenbach NS, Aye E, Han S. 2015. Functional consequences of the oligomeric assembly of proteorhodopsin. *J. Mol. Biol.* 427:1278–90



21. Sharma AK, Zhaxybayeva O, Papke RT, Doolittle WF. 2008. Actinorhodopsins: proteorhodopsin-like gene sequences found predominantly in non-marine environments. *Environ. Microbiol.* 10:1039–56
22. Balashov SP, Imasheva ES, Boichenko VA, Anton J, Wang JM, Lanyi JK. 2005. Xanthorhodopsin: a proton pump with a light-harvesting carotenoid antenna. *Science* 309:2061–64
23. Waschuk SA, Bezerra AGJ, Shi L, Brown LS. 2005. *Leptosphaeria* rhodopsin: bacteriorhodopsin-like proton pump from a eukaryote. *PNAS* 102:6879–83
24. Inoue K, Ito S, Kato Y, Nomura Y, Shibata M, et al. 2016. A natural light-driven inward proton pump. *Nat. Commun.* 7:13415
25. Matsuno-Yagi A, Mukohata Y. 1977. Two possible roles of bacteriorhodopsin; a comparative study of strains of *Halobacterium halobium* differing in pigmentation. *Biochem. Biophys. Res. Commun.* 78:237–43
26. Mukohata Y, Kaji Y. 1981. Light-induced membrane-potential increase, ATP synthesis, and proton uptake in *Halobacterium halobium*, R1mR catalyzed by halorhodopsin: effects of N,N'-dicyclohexylcarbodiimide, triphenyltin chloride, and 3,5-di-tert-butyl-4-hydroxybenzylidenemalononitrile (SF6847). *Arch. Biochem. Biophys.* 206:72–76
27. Schobert B, Lanyi JK. 1982. Halorhodopsin is a light-driven chloride pump. *J. Biol. Chem.* 257:10306–13
28. Sasaki J, Brown LS, Chon YS, Kandori H, Maeda A, et al. 1995. Conversion of bacteriorhodopsin into a chloride ion pump. *Science* 269:73–75
29. Gradinaru V, Thompson KR, Deisseroth K. 2008. eNpHR: a *Natronomonas* halorhodopsin enhanced for optogenetic applications. *Brain Cell Biol.* 36:129–39
30. Yoshizawa S, Kumagai Y, Kim H, Ogura Y, Hayashi T, et al. 2014. Functional characterization of flavobacteria rhodopsins reveals a unique class of light-driven chloride pump in bacteria. *PNAS* 111:6732–37
31. Kandori H. 2015. Ion-pumping microbial rhodopsins. *Front. Mol. Biosci.* 2:52
32. Inoue K, Koua FH, Kato Y, Abe-Yoshizumi R, Kandori H. 2014. Spectroscopic study of a light-driven chloride ion pump from marine bacteria. *J. Phys. Chem. B* 118:11190–99
33. Hosaka T, Yoshizawa S, Nakajima Y, Ohsawa N, Hato M, et al. 2016. Structural mechanism for light-driven transport by a new type of chloride ion pump, *Nonlabens marinus* rhodopsin-3. *J. Biol. Chem.* 291:17488–95
34. Hasemi T, Kikukawa T, Kamo N, Demura M. 2016. Characterization of a cyanobacterial chloride-pumping rhodopsin and its conversion into a proton pump. *J. Biol. Chem.* 291:355–62
35. Inoue K, Ono H, Abe-Yoshizumi R, Yoshizawa S, Ito H, et al. 2013. A light-driven sodium ion pump in marine bacteria. *Nat. Commun.* 4:1678
36. Kwon SK, Kim BK, Song JY, Kwak MJ, Lee CH, et al. 2013. Genomic makeup of the marine flavobacterium *Nonlabens (Donghaeana) dokdonensis* and identification of a novel class of rhodopsins. *Genome Biol. Evol.* 5:187–99
37. Balashov SP, Imasheva ES, Dioumaev AK, Wang JM, Jung KH, Lanyi JK. 2014. Light-driven Na<sup>+</sup> pump from *Gillisia limmaea*: A high-affinity Na<sup>+</sup> binding site is formed transiently in the photocycle. *Biochemistry* 53:7549–61
38. Li H, Sineschekov OA, da Silva GF, Spudich JL. 2015. In vitro demonstration of dual light-driven Na<sup>+</sup>/H<sup>+</sup> pumping by a microbial rhodopsin. *Biophys. J.* 109:1446–53
39. da Silva GF, Goblirsch BR, Tsai AL, Spudich JL. 2015. Cation-specific conformations in a dual-function ion-pumping microbial rhodopsin. *Biochemistry* 54:3950–59
40. Kato HE, Inoue K, Abe-Yoshizumi R, Kato Y, Ono H, et al. 2015. Structural basis for Na<sup>+</sup> transport mechanism by a light-driven Na<sup>+</sup> pump. *Nature* 521:48–53
41. Gushchin I, Shevchenko V, Polovinkin V, Kovalev K, Alekseev A, et al. 2015. Crystal structure of a light-driven sodium pump. *Nat. Struct. Mol. Biol.* 22:390–95
42. Spudich EN, Spudich JL. 1982. Control of transmembrane ion fluxes to select halorhodopsin-deficient and other energy-transduction mutants of *Halobacterium halobium*. *PNAS* 79:4308–12
43. Bogomolni R, Spudich JL. 1982. Identification of a third rhodopsin-like pigment in phototactic *Halobacterium halobium*. *PNAS* 79:6250–54
44. Spudich JL, Bogomolni RA. 1984. Mechanism of colour discrimination by a bacterial sensory rhodopsin. *Nature* 312:509–13

45. Berndt A, Yizhar O, Gunaydin LA, Hegemann P, Deisseroth K. 2009. Bi-stable neural state switches. *Nat. Neurosci.* 12:229–34
46. Yao VJ, Spudich JL. 1992. Primary structure of an archaeobacterial transducer, a methyl-accepting protein associated with sensory rhodopsin I. *PNAS* 89:11915–19
47. Rudolph J, Oesterhelt D. 1996. Deletion analysis of the *che* operon in the archaeon *Halobacterium salinarium*. *J. Mol. Biol.* 258:548–54
48. Takahashi T, Tomioka H, Kamo N, Kobatake Y. 1985. A photosystem other than PS370 also mediates the negative phototaxis of *Halobacterium halobium*. *FEMS Microbiol. Lett.* 28:161–64
49. Tomioka H, Takahashi T, Kamo N, Kobatake Y. 1986. Flash spectrophotometric identification of a fourth rhodopsin-like pigment in *Halobacterium halobium*. *Biochem. Biophys. Res. Commun.* 139:389–95
50. Spudich EN, Sundberg SA, Manor D, Spudich JL. 1986. Properties of a second sensory receptor protein in *Halobacterium halobium* phototaxis. *Proteins* 1:239–46
51. Luecke H, Schobert B, Lanyi JK, Spudich EN, Spudich JL. 2001. Crystal structure of sensory rhodopsin II at 2.4 angstroms: insights into color tuning and transducer interaction. *Science* 293:1499–503
52. Royant A, Nollert P, Edman K, Neutze R, Landau EM, et al. 2001. X-ray structure of sensory rhodopsin II at 2.1-Å resolution. *PNAS* 98:10131–36
53. Gordeliy VI, Labahn J, Moukhametzianov R, Efremov R, Granzin J, et al. 2002. Molecular basis of transmembrane signalling by sensory rhodopsin II-transducer complex. *Nature* 419:484–87
54. Vogeley L, Sineshchekov O, Trivedi V, Sasaki J, Spudich J, Luecke H. 2004. *Anabaena* sensory rhodopsin: a photochromic color sensor at 2.0 Å. *Science* 306:1390–93
55. Spudich JL. 1994. Protein-protein interaction converts a proton pump into a sensory receptor. *Cell* 79:747–50
56. Schmies G, Luttenberg B, Chizhov I, Engelhard M, Becker A, Bamberg E. 2000. Sensory rhodopsin II from the haloalkaliphilic *Natronobacterium pharaonis*: light-activated proton transfer reactions. *Biophys. J.* 78:967–76
57. Sudo Y, Spudich JL. 2006. Three strategically placed hydrogen-bonding residues convert a proton pump into a sensory receptor. *PNAS* 103:16129–34
58. Inoue K, Nomura Y, Kandori H. 2016. Asymmetric functional conversion of eubacterial light-driven ion pumps. *J. Biol. Chem.* 291:9883–93
59. Spudich JL, Sineshchekov OA, Govorunova EG. 2014. Mechanism divergence in microbial rhodopsins. *Biochim. Biophys. Acta* 1837:546–52
60. Jung K-H, Trivedi VD, Spudich JL. 2003. Demonstration of a sensory rhodopsin in eubacteria. *Mol. Microbiol.* 47:1513–22
61. Sineshchekov OA, Trivedi VD, Sasaki J, Spudich JL. 2005. Photochromicity of *Anabaena* sensory rhodopsin, an atypical microbial receptor with a *cis*-retinal light-adapted form. *J. Biol. Chem.* 280:14663–68
62. Irieda H, Morita T, Maki K, Homma M, Aiba H, Sudo Y. 2012. Photo-induced regulation of the chromatic adaptive gene expression by *Anabaena* sensory rhodopsin. *J. Biol. Chem.* 287:32485–93
63. Kim SY, Yoon SR, Han S, Yun Y, Jung KH. 2014. A role of *Anabaena* sensory rhodopsin transducer (ASRT) in photosensory transduction. *Mol. Microbiol.* 93:403–14
64. Wand A, Gdor I, Zhu J, Sheves M, Ruhman S. 2013. Shedding new light on retinal protein photochemistry. *Annu. Rev. Phys. Chem.* 64:437–58
65. Brown LS. 2014. Eubacterial rhodopsins—unique photosensors and diverse ion pumps. *Biochim. Biophys. Acta* 1837:553–61
66. Kateriya S, Nagel G, Bamberg E, Hegemann P. 2004. “Vision” in single-celled algae. *News Physiol. Sci.* 19:133–37
67. Kianianmomeni A, Hallmann A. 2014. Algal photoreceptors: in vivo functions and potential applications. *Planta* 239:1–26
68. Luck M, Mathes T, Bruun S, Fudim R, Hagedorn R, et al. 2012. A photochromic histidine kinase rhodopsin (HKR1) that is bimodally switched by ultraviolet and blue light. *J. Biol. Chem.* 287:40083–90
69. Penzkofer A, Luck M, Mathes T, Hegemann P. 2014. Bistable retinal Schiff base photo-dynamics of histidine kinase rhodopsin HKR1 from *Chlamydomonas reinhardtii*. *Photochem. Photobiol.* 90:773–85

70. Schmidt M, Gessner G, Luff M, Heiland I, Wagner V, et al. 2006. Proteomic analysis of the eyespot of *Chlamydomonas reinhardtii* provides novel insights into its components and tactic movements. *Plant Cell* 18:1908–30
71. Saranak J, Foster K-W. 1997. Rhodopsin guides fungal phototaxis. *Nature* 387:465–66
72. Avelar GM, Schumacher RI, Zaini PA, Leonard G, Richards TA, Gomes SL. 2014. A rhodopsin-guanylyl cyclase gene fusion functions in visual perception in a fungus. *Curr. Biol.* 24:1234–40
73. Gao S, Nagpal J, Schneider MW, Kozjak-Pavlovic V, Nagel G, Gottschalk A. 2015. Optogenetic manipulation of cGMP in cells and animals by the tightly light-regulated guanylyl-cyclase opsin CycOp. *Nat. Commun.* 6:8046
74. Avelar GM, Glaser T, Leonard G, Richards TA, Ulrich H, Gomes SL. 2015. A cGMP-dependent K<sup>+</sup> channel in the blastocladiomycete fungus *Blastocladiella emersonii*. *Eukaryot. Cell* 14:958–63
75. Scheib U, Stehfest K, Gee CE, Korsch HG, Fudim R, et al. 2015. The rhodopsin-guanylyl cyclase of the aquatic fungus *Blastocladiella emersonii* enables fast optical control of cGMP signaling. *Sci. Signal.* 8:rs8
76. Litvin FF, Sineshchekov OA, Sineshchekov VA. 1978. Photoreceptor electric potential in the phototaxis of the alga *Haematococcus pluvialis*. *Nature* 271:476–78
77. Foster K-W, Saranak J, Patel N, Zarrilli G, Okabe M, et al. 1984. A rhodopsin is the functional photoreceptor for phototaxis in the unicellular eukaryote *Chlamydomonas*. *Nature* 311:756–59
78. Sineshchekov OA, Jung K-H, Spudich JL. 2002. Two rhodopsins mediate phototaxis to low- and high-intensity light in *Chlamydomonas reinhardtii*. *PNAS* 99:8689–94
79. Nagel G, Ollig D, Fuhrmann M, Kateriya S, Musti AM, et al. 2002. Channelrhodopsin-1: a light-gated proton channel in green algae. *Science* 296:2395–98
80. Nagel G, Szellas T, Huhn W, Kateriya S, Adeishvili N, et al. 2003. Channelrhodopsin-2, a directly light-gated cation-selective membrane channel. *PNAS* 100:13940–45
81. Boyden ES, Zhang F, Bamberg E, Nagel G, Deisseroth K. 2005. Millisecond-timescale, genetically targeted optical control of neural activity. *Nat. Neurosci.* 8:1263–68
82. Govorunova EG, Sineshchekov OA, Liu X, Janz R, Spudich JL. 2015. Natural light-gated anion channels: a family of microbial rhodopsins for advanced optogenetics. *Science* 349:647–50
83. Sineshchekov OA, Spudich JL. 2005. Sensory rhodopsin signaling in green flagellate algae. In *Handbook of Photosensory Receptors*, ed. WR Briggs, JL Spudich, pp. 25–42. Weinheim, Ger.: Wiley-VCH
84. Sineshchekov OA, Litvin FF, Keszthelyi L. 1990. Two components of photoreceptor potential of the flagellated green alga *Haematococcus pluvialis*. *Biophys. J.* 57:33–39
85. Sineshchekov OA, Govorunova EG, Spudich JL. 2009. Photosensory functions of channelrhodopsins in native algal cells. *Photochem. Photobiol.* 85:556–63
86. Govorunova EG, Jung K-W, Sineshchekov OA, Spudich JL. 2004. *Chlamydomonas* sensory rhodopsins A and B: cellular content and role in photophobic responses. *Biophys. J.* 86:2342–49
87. Klapoetke NC, Murata Y, Kim SS, Pulver SR, Birdsey-Benson A, et al. 2014. Independent optical excitation of distinct neural populations. *Nat. Methods* 11:338–46
88. Schneider F, Grimm C, Hegemann P. 2015. Biophysics of channelrhodopsin. *Annu. Rev. Biophys.* 44:167–86
89. Kato HE, Zhang F, Yizhar O, Ramakrishnan C, Nishizawa T, et al. 2012. Crystal structure of the channelrhodopsin light-gated cation channel. *Nature* 482:369–74
90. Bruun S, Stoeppler D, Keidel A, Kuhlmann U, Luck M, et al. 2015. Light-dark adaptation of channelrhodopsin involves photoconversion between the all-*trans* and 13-*cis* retinal isomers. *Biochemistry* 54:3389–400
91. Lorenz-Fonfria VA, Schultz BJ, Resler T, Schlesinger R, Bamann C, et al. 2015. Pre-gating conformational changes in the ChETA variant of channelrhodopsin-2 monitored by nanosecond IR spectroscopy. *J. Am. Chem. Soc.* 137:1850–61
92. Ernst OP, Sanchez Murcia PA, Daldrop P, Tsunoda SP, Kateriya S, Hegemann P. 2008. Photoactivation of channelrhodopsin. *J. Biol. Chem.* 283:1637–43
93. Verhoeven MK, Bamann C, Blocher R, Forster U, Bamberg E, Wachtveitl J. 2010. The photocycle of channelrhodopsin-2: ultrafast reaction dynamics and subsequent reaction steps. *ChemPhysChem* 11:3113–22

94. Szundi I, Li H, Chen E, Bogomolni R, Spudich JL, Kliger DS. 2015. *Platymonas subcordiformis* channelrhodopsin-2 function: I. The photochemical reaction cycle. *J. Biol. Chem.* 290:16573–84
95. Bamann C, Kirsch T, Nagel G, Bamberg E. 2008. Spectral characteristics of the photocycle of channelrhodopsin-2 and its implication for channel function. *J. Mol. Biol.* 375:686–94
96. Ritter E, Stehfest K, Berndt A, Hegemann P, Bartl FJ. 2008. Monitoring light-induced structural changes of channelrhodopsin-2 by UV-visible and Fourier transform infrared spectroscopy. *J. Biol. Chem.* 283:35033–41
97. Sineshchekov OA, Govorunova EG, Wang J, Li H, Spudich JL. 2013. Intramolecular proton transfer in channelrhodopsins. *Biophys. J.* 104:807–17
98. Lorenz-Fonfria VA, Resler T, Krause N, Nack M, Gossing M, et al. 2013. Transient protonation changes in channelrhodopsin-2 and their relevance to channel gating. *PNAS* 110:E1273–81
99. Ogren JI, Yi A, Mamaev S, Li H, Spudich JL, Rothschild KJ. 2015. Proton transfers in a channelrhodopsin-1 studied by FTIR-difference spectroscopy and site-directed mutagenesis. *J. Biol. Chem.* 290:12719–30
100. Kuhne J, Eisenhauer K, Ritter E, Hegemann P, Gerwert K, Bartl F. 2014. Early formation of the ion-conducting pore in channelrhodopsin-2. *Angew. Chem. Int. Ed. Engl.* 54:4953–57
101. Resler T, Schultz BJ, Lorenz-Fonfria VA, Schlesinger R, Heberle J. 2015. Kinetic and vibrational isotope effects of proton transfer reactions in channelrhodopsin-2. *Biophys. J.* 109:287–97
102. Nack M, Radu I, Gossing M, Bamann C, Bamberg E, et al. 2010. The DC gate in channelrhodopsin-2: crucial hydrogen bonding interaction between C128 and D156. *Photochem. Photobiol. Sci.* 9:194–98
103. Bamann C, Gueta R, Kleinlogel S, Nagel G, Bamberg E. 2010. Structural guidance of the photocycle of channelrhodopsin-2 by an interhelical hydrogen bond. *Biochemistry* 49:267–78
104. Ritter E, Piwowarski P, Hegemann P, Bartl FJ. 2013. Light-dark adaptation of channelrhodopsin C128T mutant. *J. Biol. Chem.* 288:10451–58
105. Stehfest K, Hegemann P. 2010. Evolution of the channelrhodopsin photocycle model. *ChemPhysChem* 11:1120–26
106. Radu I, Bamann C, Nack M, Nagel G, Bamberg E, Heberle J. 2009. Conformational changes of channelrhodopsin-2. *J. Am. Chem. Soc.* 131:7313–19
107. Neumann-Verhoeven MK, Neumann K, Bamann C, Radu I, Heberle J, et al. 2013. Ultrafast infrared spectroscopy on channelrhodopsin-2 reveals efficient energy transfer from the retinal chromophore to the protein. *J. Am. Chem. Soc.* 135:6968–76
108. Krause N, Engelhard C, Heberle J, Schlesinger R, Bittl R. 2013. Structural differences between the closed and open states of channelrhodopsin-2 as observed by EPR spectroscopy. *FEBS Lett.* 587:3309–13
109. Sattig T, Rickert C, Bamberg E, Steinhoff HJ, Bamann C. 2013. Light-induced movement of the transmembrane helix B in channelrhodopsin-2. *Angew. Chem. Int. Ed. Engl.* 52:9705–8
110. Volz P, Krause N, Balke J, Schneider C, Walter M, et al. 2016. Light and pH-induced changes in structure and accessibility of transmembrane helix B and its immediate environment in channelrhodopsin-2. *J. Biol. Chem.* 291:17382–93
111. Müller M, Bamann C, Bamberg E, Kuhlbrandt W. 2015. Light-induced helix movements in channelrhodopsin-2. *J. Mol. Biol.* 427:341–49
112. Subramaniam S, Gerstein M, Oesterheld D, Henderson R. 1993. Electron diffraction analysis of structural changes in the photocycle of bacteriorhodopsin. *EMBO J.* 12:1–8
113. Sasaki J, Tsai AL, Spudich JL. 2011. Opposite displacement of helix F in attractant and repellent signaling by sensory rhodopsin-Htr complexes. *J. Biol. Chem.* 286:18868–77
114. Wegener AA, Chizhov I, Engelhard M, Steinhoff HJ. 2000. Time-resolved detection of transient movement of helix F in spin-labelled pharaonis sensory rhodopsin II. *J. Mol. Biol.* 301:881–91
115. Lorenz-Fonfria VA, Bamann C, Resler T, Schlesinger R, Bamberg E, Heberle J. 2015. Temporal evolution of helix hydration in a light-gated ion channel correlates with ion conductance. *PNAS* 112:E5796–804
116. Eisenhauer K, Kuhne J, Ritter E, Berndt AE, Wolf S, et al. 2012. In channelrhodopsin-2 E90 is crucial for ion selectivity and is deprotonated during the photocycle. *J. Biol. Chem.* 287:6904–11
117. Feldbauer K, Zimmermann D, Pintschovius V, Spitz J, Bamann C, Bamberg E. 2009. Channelrhodopsin-2 is a leaky proton pump. *PNAS* 106:12317–22

118. Govorunova EG, Sineshchekov OA, Li H, Janz R, Spudich JL. 2013. Characterization of a highly efficient blue-shifted channelrhodopsin from the marine alga *Platymonas subcordiformis*. *J. Biol. Chem.* 288:29911–22
119. Schneider F, Gradmann D, Hegemann P. 2013. Ion selectivity and competition in channelrhodopsins. *Biophys. J.* 105:91–100
120. Zhao M, Alleva R, Ma H, Daniel AG, Schwartz TH. 2015. Optogenetic tools for modulating and probing the epileptic network. *Epilepsy Res.* 116:15–26
121. Cohen AE. 2016. Optogenetics: turning the microscope on its head. *Biophys. J.* 110:997–1003
122. Wietek J, Prigge M. 2016. Enhancing channelrhodopsins: an overview. *Methods Mol. Biol.* 1408:141–65
123. Lin JY, Knutsen PM, Muller A, Kleinfeld D, Tsien RY. 2013. ReaChR: A red-shifted variant of channelrhodopsin enables deep transcranial optogenetic excitation. *Nat. Neurosci.* 16:1499–508
124. Kato HE, Kamiya M, Sugo S, Ito J, Taniguchi R, et al. 2015. Atomistic design of microbial opsin-based blue-shifted optogenetics tools. *Nat. Commun.* 6:7177
125. Kleinlogel S, Feldbauer K, Dempski RE, Fotis H, Wood PG, et al. 2011. Ultra light-sensitive and fast neuronal activation with the Ca<sup>2+</sup>-permeable channelrhodopsin CatCh. *Nat. Neurosci.* 14:513–18
126. Lin JY. 2010. A user's guide to channelrhodopsin variants: features, limitations and future developments. *Exp. Physiol.* 96:19–25
127. Yizhar O, Fenno LE, Davidson TJ, Mogri M, Deisseroth K. 2011. Optogenetics in neural systems. *Neuron* 71:9–34
128. Mattis J, Tye KM, Ferenczi EA, Ramakrishnan C, O'Shea DJ, et al. 2011. Principles for applying optogenetic tools derived from direct comparative analysis of microbial opsins. *Nat. Methods* 9:159–72
129. Mohanty SK, Reinscheid RK, Liu X, Okamura N, Krasieva TB, Berns MW. 2008. In-depth activation of channelrhodopsin 2-sensitized excitable cells with high spatial resolution using two-photon excitation with a near-infrared laser microbeam. *Biophys. J.* 95:3916–26
130. Grubb MS, Burrone J. 2010. Channelrhodopsin-2 localised to the axon initial segment. *PLOS ONE* 5:e13761
131. Hochbaum DR, Zhao Y, Farhi SL, Klapoetke N, Werley CA, et al. 2014. All-optical electrophysiology in mammalian neurons using engineered microbial rhodopsins. *Nat. Methods* 8:825–33
132. Sineshchekov OA, Govorunova EG, Jung K-H, Zauner S, Maier U-G, Spudich JL. 2005. Rhodopsin-mediated photoreception in cryptophyte flagellates. *Biophys. J.* 89:4310–19
133. Govorunova EG, Sineshchekov OA, Spudich JL. 2016. *Proteomonas sulcata* ACR1: a fast anion channelrhodopsin. *Photochem. Photobiol.* 92:257–63
134. Wietek J, Broser M, Krause BS, Hegemann P. 2016. Identification of a natural green light absorbing chloride conducting channelrhodopsin from *Proteomonas sulcata*. *J. Biol. Chem.* 291:4121–27
135. Keeling PJ, Burki F, Wilcox HM, Allam B, Allen EE, et al. 2014. The Marine Microbial Eukaryote Transcriptome Sequencing Project (MMETSP): illuminating the functional diversity of eukaryotic life in the oceans through transcriptome sequencing. *PLOS Biol.* 12:e1001889
136. Matasci N, Hung LH, Yan Z, Carpenter EJ, Wickett NJ, et al. 2014. Data access for the 1,000 Plants (1KP) project. *Gigascience* 3:17
137. Sineshchekov OA, Li H, Govorunova EG, Spudich JL. 2016. Photochemical reaction cycle transitions during anion channelrhodopsin gating. *PNAS* 113:E1993–2000
138. Zhang F, Vierock J, Yizhar O, Fenno LE, Tsunoda S, et al. 2011. The microbial opsin family of optogenetic tools. *Cell* 147:1446–57
139. Wietek J, Wiegert JS, Adeishvili N, Schneider F, Watanabe H, et al. 2014. Conversion of channelrhodopsin into a light-gated chloride channel. *Science* 344:409–12
140. Sineshchekov OA, Govorunova EG, Li H, Spudich JL. 2015. Gating mechanisms of a natural anion channelrhodopsin. *PNAS* 112:14236–41
141. Wietek J, Beltramo R, Scanziani M, Hegemann P, Oertner TG, Simon WJ. 2015. An improved chloride-conducting channelrhodopsin for light-induced inhibition of neuronal activity in vivo. *Sci. Rep.* 5:14807
142. Berndt A, Lee SY, Ramakrishnan C, Deisseroth K. 2014. Structure-guided transformation of channelrhodopsin into a light-activated chloride channel. *Science* 344:420–24
143. Berndt A, Lee SY, Wietek J, Ramakrishnan C, Steinberg EE, et al. 2015. Structural foundations of optogenetics: determinants of channelrhodopsin ion selectivity. *PNAS* 113:822–29



144. Berndt A, Deisseroth K. 2015. Expanding the optogenetics toolkit. *Science* 349:590–91
145. Olson KD, Zhang XN, Spudich JL. 1995. Residue replacements of buried aspartyl and related residues in sensory rhodopsin I: D201N produces inverted phototaxis signals. *PNAS* 92:3185–89
146. Jung KH, Spudich JL. 1998. Suppressor mutation analysis of the sensory rhodopsin I-transducer complex: insights into the color-sensing mechanism. *J. Bacteriol.* 180:2033–42
147. Sineshchekov OA, Sasaki J, Phillips BJ, Spudich JL. 2008. A Schiff base connectivity switch in sensory rhodopsin signaling. *PNAS* 105:16159–64
148. Sineshchekov OA, Sasaki J, Wang J, Spudich JL. 2010. Attractant and repellent signaling conformers of sensory rhodopsin-transducer complexes. *Biochemistry* 49:6696–704
149. Sasaki J, Takahashi H, Furutani Y, Kandori H, Spudich JL. 2011. Sensory rhodopsin-I as a bidirectional switch: opposite conformational changes from the same photoisomerization. *Biophys. J.* 100:2178–83
150. Yi A, Mamaeva NV, Li H, Spudich JL, Rothschild KJ. 2016. Resonance Raman study of an anion channelrhodopsin: effects of mutations near the retinylidene Schiff base. *Biochemistry* 55:2371–80
151. Kolbe M, Besir H, Essen LO, Oesterhelt D. 2000. Structure of the light-driven chloride pump halorhodopsin at 1.8 angstrom resolution. *Science* 288:1390–96
152. Mahn M, Prigge M, Ron S, Levy R, Yizhar O. 2016. Biophysical constraints of optogenetic inhibition at presynaptic terminals. *Nat. Neurosci.* 19:554–56
153. Mohammad F, Stewart J, Ott S, Chlebikova K, Chua JI, et al. 2017. Optogenetic inhibition of behavior with anion channelrhodopsins. *Nat. Methods* 14:271–74
154. Alfonsa H, Lakey JH, Lightowlers RN, Trevelyan AJ. 2016. Cl-out is a novel cooperative optogenetic tool for extruding chloride from neurons. *Nat. Commun.* 7:13495
155. Govorunova EG, Cunha CR, Sineshchekov OA, Spudich JL. 2016. Anion channelrhodopsins for inhibitory cardiac optogenetics. *Sci. Rep.* 6:33530
156. Govorunova EG, Sineshchekov OA, Spudich JL. 2016. Structurally distinct cation channelrhodopsins from cryptophyte algae. *Biophys. J.* 110:2302–4
157. Brown LS, Dioumaev AK, Lanyi JK, Spudich EN, Spudich JL. 2001. Photochemical reaction cycle and proton transfers in *Neurospora* rhodopsin. *J. Biol. Chem.* 276:32495–505
158. Li H, Sineshchekov OA, Wu G, Spudich JL. 2016. In vitro activity of a purified natural anion channelrhodopsin. *J. Biol. Chem.* 291:25319–25
159. Watanabe M, Furuya M. 1974. Action spectrum of phototaxis in a cryptomonad alga, *Cryptomonas* sp. *Plant Cell Physiol.* 15:413–20
160. Yue L, Weiland JD, Roska B, Humayun MS. 2016. Retinal stimulation strategies to restore vision: fundamentals and systems. *Prog. Retin. Eye Res.* 53:21–47
161. Doroudchi MM, Greenberg KP, Liu J, Silka KA, Boyden ES, et al. 2011. Virally delivered channelrhodopsin-2 safely and effectively restores visual function in multiple mouse models of blindness. *Mol. Ther.* 19:1220–29
162. Govorunova EG, Sineshchekov OA, Rodarte EM, Janz R, Morelle O, et al. 2017. The expanding family of natural anion channelrhodopsins reveals large variations in kinetics, conductance, and spectral sensitivity. *Sci. Rep.* 7:43358